Università degli Studi di Salerno

Dipartimento di ingegneria dell'Informazione ed
Elettrica e Matematica applicata

Ph.D. Program in Information Engineering

First year report

Author:
dott. Francesco Rosa

Supervisor:
Ch.mo. Mario Vento

XXXVII cycle - Academic year 2021/2022

Contents

Overview

This report represents the final document of the first year of the doctorate carried out by the undersigned. The document conforms to the latest version of the document *"Requirements for the PhD degree"* approved on 14/12/2020 by the professors' college and available on the university platform in the area reserved for doctoral students. As requested, the document contains a report on the activities carried out by the student during the first year.

The document is divided, as suggested, in the aforementioned document, into 3 mandatory chapters, Background 1, Research Plan 2, and Other Activities 3.
The first chapter contains the Introduction (Section 1.1) and the State-of-the-Art (Section 1.2) sections. The former introduces to the topic of *Learning from Demonstration*, that is the main topic of this report, pointing out the the importance of the field and the existing knowledge. The latter presents the literature review. This section analyzes from a methodological and application perspective the main approaches by which the problem is solved, highlighting the pros and cons of each method.
The second chapter containes the Research Gaps (Section **??**) and the Research Plan (Section 2.2) sections. The first presents the gaps that can be extrapolated from the State-of-the-Art, with respect to the context of interest. The second reports the proposed research activity, going on to highlight the connection between the proposal and the gaps presented earlier, the importance of the proposal with respect to the context of interest, and the methodological and experimental procedures that will be followed to track and evaluate progress.
The third chapter shows all the activities carried out during the year, including courses attended at the university, both mandatory and not.

Chapter 1

Background

1.1 Introduction

Robot technology is one of the pillars of modern society. Thanks to advances in information, electronic, and mechanical fields, we can build and program machines to solve various tasks in different scenarios, e.g. industrial, surgery, space missions etc.
In manufacturing, given their ability to reproduce the same movement over time with an high level of accuracy and precision, robots are massively used to solve repetitive and dangerous activities such as assembly, welding (Figure 1.1a) and material handling (Figure 1.1b).

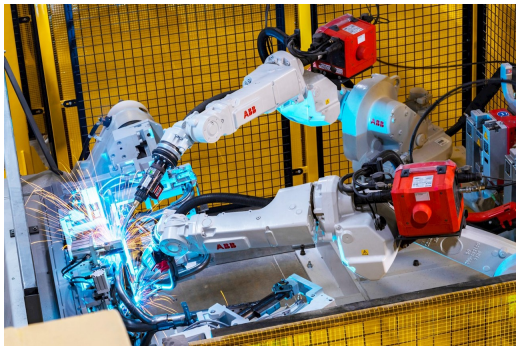

(a) Robots involved in arc welding operation

(b) Robot involved in loading operation

Figure 1.1: Industrial Robots: example of applications

While in the early day, robot systems were constrained in isolated and known environments. Over the past few decades, robots have been asked to solve tasks in dynamic and unknown/partially-known environments, where they must **coexist** and **cooperate** with humans, while solving different **dynamic** tasks (e.g. pick a requested object, whose position is not known a priori).
The reason for the increasing demand for such applications may be found in factors such as:

(a) The affirmation of the *Industry 4.0* paradigm, in which the various phases of a factory are linked to each other and therefore the robots must be in communication with each other and be able to adapt to changes in the production phases.

(b) The spreading of *social robots* (e.g. Pepper [1]), that find their appeal in highly unstructured applications such as household or shop-recommendation systems.

(c) The increasing availability of the so-called *cobots* (e.g. Franka Emika Panda robot [2]), which are low-cost robots that allow the automation of light load processes (e.g. drilling, palletizing, polishing) while sharing the workspace with humans or other robots. Thanks to cobots, also small factories, that were left out from this automation process because of the high-cost of previous solutions, can now start to automate their production phases, contributing to increase the demand.

In this scenario, the desired characteristics of such robotic systems are: **(a) Adaptability to new conditions**, i.e., the system must be able to easly adapt to dynamc change in system and environmental conditions (e.g, motor failure or a different ground's coefficient of friction for a quadruped robot [3]), performing *"intelligent" behaviors* to handle these new scenarios and solve the desired task; **(b) Adaptability to new tasks**, i.e., the system must be able to easly adapt to both new variations of a known task (e.g., new objects and different initial conditions [4]) and completely new tasks [5] by exploiting past experience to infer actions and solve them; **(c) Reliability**, i.e., the proposed system must be reliable in terms of success rate (tasks must be solved with a success rate that is reasonable for a real-world application), and safety (actions must not harm the environment, people, or the robot itself); **(d) Computation efficiency**, i.e., the system must meet all the constraints above and run in real-time on real-world robot platforms as efficiently as possible.
These requirements, especially **(a)-(b)**, can be difficult to obtain with typical robot programming techniques based on hand-written policy, and control techniques which require a careful analysis of the process dynamics, the building of an analytic model, and finally, the derivation of a control law that meets certain design criteria [6]. This design process is tedious, and time consuming, especially when **high-level perception systems** (e.g. camera, microphones, motion sensors etc.) are used to infer the state of the environment (e.g. the unknown position of the desired object to pick with respect to the end-effector) and the intention of the human operator.
In contrast, very relevant results have been obtained by leveraging *Learning Techniques*, which exploit **agent experience** or **expert demonstration**. Generally, the former is referred as *Reinforcement Learning* (RL) [7], while the latter is referred as *Imitation Learning* (IL) or *Learning from Demonstration* (LfD) [8]. Both the approaches aim to obtain an artificial agent, that is able to perform correctly a task or a set of tasks by following a learned policy, however the way how this goal is achieved is quite different. The main differences between RL and IL are related to presence/absence of a reward function, and the presence/absence of expert demonstrations.
Indeed, in RL formalism [9], the learning procedure is based on a *hand-designed reward function*, i.e., a measure of the quality of the performed action with respect to the task to be executed (e.g., the distance between the current position and the target one in a reaching task), which drives the agent to produce a sequence of actions which maximize the reward. While in IL formalism [10], the learning procedure is based on the minimization of a *loss-function* (e.g. Mean-Squared Error [11], Hinge-loss [12], Kullback-Leibler divergence [13]), which guides the agent to reproduce/mimic the same actions of the expert.
Regarding the possibility to exploit past experience, in RL literature, three approaches can be found [14]:

- ***On-policy*** Reinforcement Learning (Figure 1.2a), the trained policy is the same policy used to collect data, and the only used past experience is related to the last

policy rollout. Generally, this approach can lead to data inefficiency problems.

- ***Off-policy*** Reinforcement Learning (Figure 1.2b), in this setting there are two policies, the behavior policy used to collect data, and the learned target policy. The latter is improved during the training by leveraging past experience contained in the dynamic buffer $\mathcal{D}$, which is updated after each iteration by adding new samples collected through the behavior policy.

- ***Offline*** Reinforcement Learning (Figure 1.2c), this setting is strictly related to the classic *supervised learning approach*. The target policy is trained by exploiting a *static dataset* D, collected by an unknown policy π_β. Unlike previous methods, the training procedure requires no further interaction with the environment, and despite strong theoretical results, which can lead to prefer offline RL over behavioral cloning [15], when these algorithms are applied in robot manipulation tasks with sparse-reward and high-dimensional high-level state representation (e.g., robot images), they perform poorly with respect to classic behavioral cloning [16].

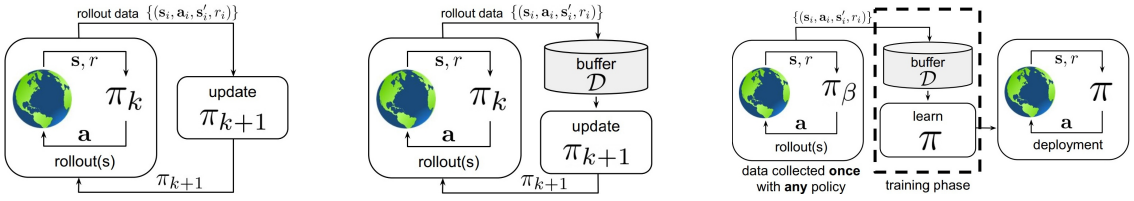

(a) On-policy RL *(b) Off-policy RL* *(c) Offline RL*

Figure 1.2: Graphical Representation of Reinforcement Learning Methods [14]

The need for both a task-specific reward function and expensive time-consuming training procedures are the main difficulties in applying such methods for real-world application [17].
As opposed to RL, in IL, the starting point for all the methods (Figure 1.3), is a dataset D containing expert demonstrations (e.g. trajectories of teleoperated robot, video of human performing a task). Based on the approach, the information contained in the dataset is used in different way:

- ***Behavioral Cloning*** (BC), the information contained in the dataset is used as *ground truth*, i.e., the final learned policy mimics the same actions in the dataset.

- ***Inverse Reinforcement Learning*** (IRL), the demonstrations are used to learn a *cost function*, that is subsequently used by an RL algorithm.

- ***Generative Adversarial Imitation Learning*** (GAIL), combination of Generative Adversarial Learning and Imitation Learning. In this setting the agent, which acts as generator, must produce a sequence of state transitions, such that a discriminator is not able to distinguish between transitions generated by the agent, and the ones generated by the expert and contained in the dataset.

- ***Learning from Observation*** (LfO), inspired by the fact that humans and animals are able to learn by just watching a demonstrator, without knowing the underlaying performed actions (e.g., the joint position), here, the aim of the artificial agent is to reproduce the observed behavior, starting from state-only demonstrations [18].

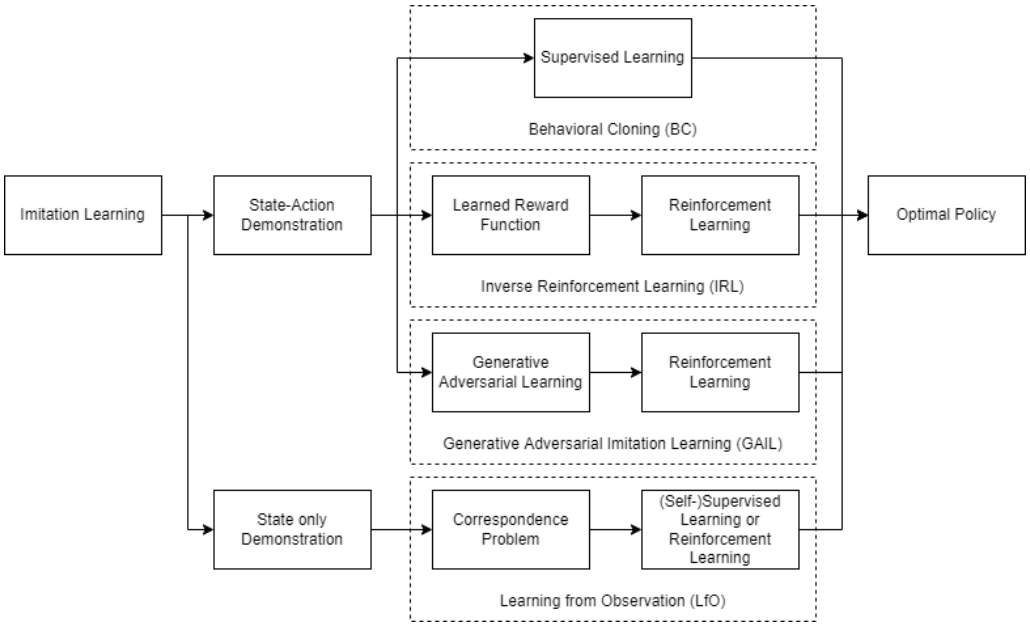

Figure 1.3: Imitation Learning: Taxonomy and main components

From Figure 1.3, it can be noted as IL and RL are strictly related, indeed, RL algorithms are used in the training procedure of some approaches, such as IRL, GAIL, and LfO. However, with respect to classic RL, IL allows to: **(1)** bypass, or at least attenuate, the time-consuming exploration that would be required in a pure RL setting, since the demonstrations are used to "guide" the exploration; **(2)** communicate, through demonstrations, a "preference" for how a task should be performed; **(3)** describe concepts that may be difficult to define formally or programmatically. As will be explained in detail in Section 1.2, BC methods suffers of the *compounding error* problem, since the i.i.d. assumption that lays behind Supervised Learning is violated. IRL was proposed to combine both the data-efficiency of IL, to learn a reward function given the samples, and the exploration capability of RL, to attenuate the *compounding error* problem. However, methods, based on this approach, have proved difficult to train. GAIL was proposed to reduce the training complexity related to IRL, by framing the IRL problem as an Adversarial Learning problem. While the GAIL based methods improved both the performance and the efficiency w.r.t. IRL methods, they showed poor performance when applied in high-dimensional data, mainly due to the *casual-confusion* problem. LfO was mainly proposed with the aim to find a way to exploit state-only demonstrations (e.g., video of humans performing a task), that are easy to collect. However, since there is not any information about the true action, a way to measure the quality of prediction is needed. Moreover, the *correspondence problem*, i.e., how to map demonstrations given in a space different from the robot one into the corresponding action in the robot space, must be solved.
Despite all the presented open-challenges, IL was successfully applied for solving complex tasks, such as driving a toy car [19], pick-and-place [20], and collaborative toolbox assembly [21], highlighting the high potential of such methods, which may justify an effort in an attempt to resolve the gaps presented. A detailed description of the mentioned approaches will be given in *Section* 1.2, with an exhaustive comparison and description of the most recent and relevant methods.

1.2 State-of-the-Art

The chapter reviews the State-of-the-Art related to the *Learning from Demonstration* problem. It will start with a general problem formulation (Section 1.2.1). Then it will briefly present the different methods used to collect data (Section 1.2.2). Next, the proposed methods will be explained and compared (Section 1.2.3). In the end, a summary will be presented, where a cross-approach comparison will be performed, and the current challenges will be emphasized (Section 1.2.4).

1.2.1 Problem Definition

Imitation Learning aims to obtain an agent that can replicate the behavior demonstrated by an expert agent. The behavior is described by a **policy**, where π^L defines the learned policy, and π^E defines the expert one. In the broadest possible definition, π^L is obtained starting from a dataset $\mathcal{D} = \{(\boldsymbol{\tau}_i, \boldsymbol{c}_i)\}_i^N$, where:

- $\boldsymbol{\tau}_i$ is the i^{th} demonstrated trajectory, which can be described as:
  - A state-action sequence, i.e., $\boldsymbol{\tau}_i = [s_0, a_0, \dots, s_T, a_T]$, when it is assumed to have access to the ground-truth action performed by the expert.
  - A state sequence, i.e., $\boldsymbol{\tau}_i = [s_0, \dots, s_T]$, when it is assumed to not have access to the ground-truth action.
- $\boldsymbol{c}_i$ is the *context-vector*, it contains task-related information, e.g. the initial state of the system s_0, or the position of the target object.

The policy π^L can be defined with respect to different abstraction levels [22, 10]: (**a**) *Symbolic Characterization*, the policy maps states, and context to a sequence of options, i.e., $\pi : s_t, \mathbf{c} \rightarrow [o_1, \dots, o_T]$, where each option is a sequence of actions. With this representation, complex tasks can be decomposed into a sequence of simple movements. However, it is hard to achieve an accurate task segmentation and motion ordering; (**b**) *Trajectory Characterization*, the policy maps context to trajectory, i.e., $\pi : \mathbf{c} \rightarrow \boldsymbol{\tau}$. Because it allows the initial state to be mapped to a complete sequence of actions, this representation can be used to obtain the options in the Symbolic Representation. However, they need as many dynamic features as possible, that can be difficult to obtain; (**c**) *State-Action Characterization*, the policy maps states(-context) to actions, i.e., $\pi : s_t, \mathbf{c} \rightarrow a_t$. This representation makes it possible to map the current state directly to the corresponding action. However, it is easy for errors to accumulate in long-term processes.
The agent, by means of its policy π, acts on a system, which is modeled as a *Markov Decision Process* (MDP) [23]. A MDP is defined as a tuple (S, A, R, T, γ), where:

- $S \subseteq \mathbb{R}^n$, is a set of states (e.g. joints position and/or image).
- $A \subseteq \mathbb{R}^n$, is a set of actions, (e.g. desired end-effector pose, desired joints torque).
- $R(s, a, s')$, is a *reward function*, which expresses the immediate reward for executing action a in state s, and transitioning to state s'.
- $T(s'|s, a)$ is a *transition function*, which defines the probability to reach the state s', after the execution of action a in state s. This distribution, which describe the *system dynamic*, can be given a priori or learned (Model-Based methods), or do not taken into account (Model-Free methods).

- $\gamma \in [0, 1]$, is a discount factor expressing the agent's preference for immediate over future rewards.

With respect to the given MDP definition, the reward function plays different roles based on the used approach. Indeed, in BC methods, the reward function is not implicitly used, but a surrogate loss-function is used instead. In IRL the reward function is learned, assuming that the expert acts (near-)optimal w.r.t. some unknown reward function. In GAIL and LfO, the rule played by the reward function is different based on the specific method, as will be explained in Section 1.2.3.

1.2.2 Source of Demonstration

Regarding the way how the expert demonstrations can be obtained, according to [22], two categories can be identified: **(a)** direct demonstration; **(b)** indirect demonstration.

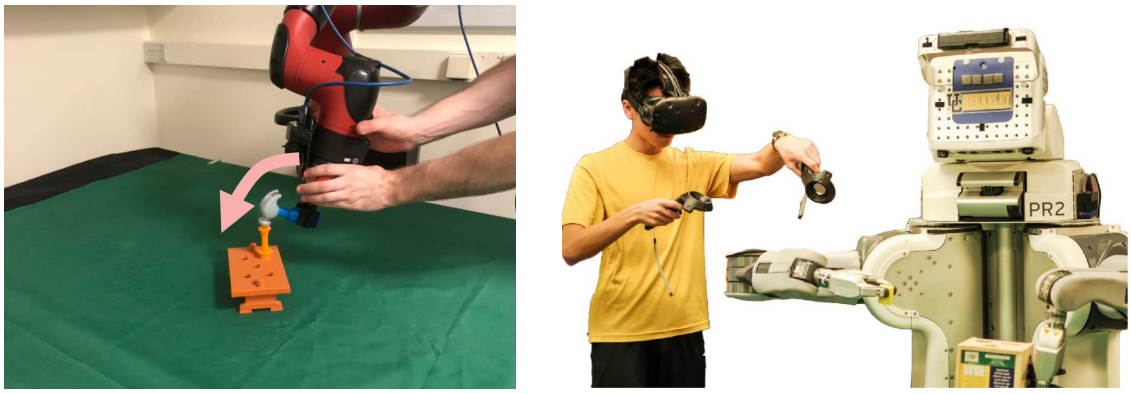

(a) Example of kinesthetic teaching [24] *(b) Example of teleoperation [20]*

Figure 1.4: Examples of Direct Demonstration

Direct Demonstration
It allows samples to be directly obtained from the robot, either with kinesthetic teaching (Figure 1.4a) or teleoperation teaching (Figure 1.4b). In kinesthetic teaching the human operator contacts and guides the robot, that collects data by itself, while in teleoperation teaching the human operator remotely guides the robot with joystick, control panel, and wearable device. The former is characterized by the fact that there is no need to consider difference in kinematic between human and robot, as consequence, data has less noise. However, the robot must be passively controllable and require direct contact, introducing safety problems, and unintuitive demonstrations for robot with multiple degrees of freedom. The latter is characterized by a higher safety, since there is no direct contact, and a wide application range. A very popular example of teleoperation system is *Roboturk* [25]. It is a cloud-based teleoperation framework that enables the collection of high-scale demonstration dataset [26, 16], for both simulated and real-world robots, using a mobile-phone as controller (Figure 1.5). While this framework is interesting since it allows to collect data from a wide range of demonstrator with different demonstrations quality, it lacks of tactile information. When data are collected employing teleoperation, a way to collect contact information between the robot and the environment is represented by haptic interfaces [27, 28], which would allow the human operator to receive a force-feedback during teleoperation. However, the current literature has not yet focused on exploiting

haptic information in the context of Learning from Demonstration, mainly due to the presence of open-challenges related to exploiting and best representing robot motion-related information, as will be explained in the following sections.

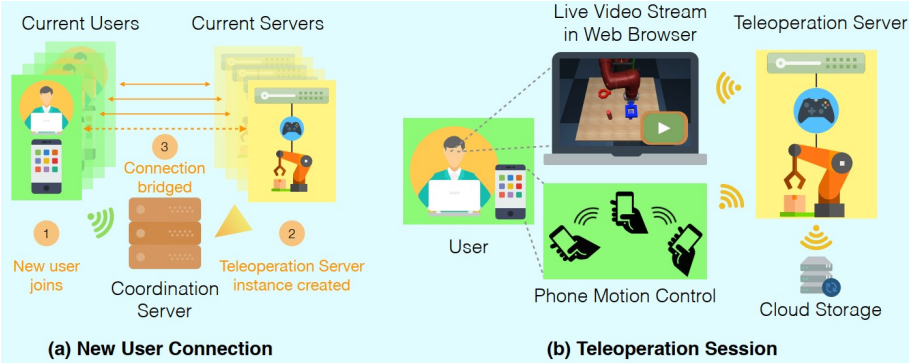

Figure 1.5: System diagram of Roboturk [25]

Indirect Demonstration
It allows samples to be acquired in a way that is completely disconnected from the robot platform. In this case the human motion is recorded by vision system [29, 30] or wearable device [31]. In last years, the ability to extrapolate a policy starting from video of human performing a task has become a very important topic in the current literature [22, 18]. While Indirect Demonstration based on visual system allows to collect samples in the most intuitive and scalable way possible (potentially any video of performed task can be used), it lacks of tactile information, which can be obtained by using wearable devices such as gloves endowed with sensors able to measure the contact forces [32]. However, the correspondence problem must be solved, i.e., the system must be able to map motion captured in human space into the corresponding motion of the robot. In Section 1.2.3, the different ways this problem has been solved in the context of visual demonstration will be explained in detail.

1.2.3 Methods

In this section the different methods used to solve the Learning from Demonstration problem are presented. The paragraphs are organized according to the temporal order in which the different approaches were proposed for the context of interest. So the first paragraph will be devoted to methods related to Behavioral Cloning. A brief presentation will be made on methods related to Inverse Reinforcement Learning. In conclusion, recent methods related to Generative Adversarial Imitation Learning and Learning from Observation will be described and analyzed.

Behavioral Cloning (BC).
Behavioral Cloning is one of the first approach used to learn a task from a set of demonstrations. Generally, it is framed as a Supervised Learning problem. Algorithm 1 defines the classic procedure used to solve the learning task, where, given the dataset $\mathcal{D}^E$, a parameterized learner policy π_θ^L, and a loss-function $\mathcal{L}$, the goal is to find the policy's parameter that minimizes the loss-function, or in other terms, $\theta^* = \underset{\theta}{argmin}\, \mathbb{E}_{(\boldsymbol{\tau},\mathbf{c})\sim\mathcal{D}^E}\,[\mathcal{L}((\boldsymbol{\tau},\mathbf{c}),\, \pi_\theta^L)]$.

In this setting there are at least two questions to answer: **(1)** choose whether to optimize in trajectory space or action space; **(2)** what kind of representation to use for the policy. According to [10], BC methods can be categorized as Model-Free and Model-Based. Moreover, a further classification can be based on the fact that the policy is optimized either in the *trajectory space* or in the *action space*.

Algorithm 1 Abstract Algorithm for Behavioral Cloning

Require: A set of expert demonstrations $\mathcal{D}^E$, a parameterized policy π_θ^L
Ensure: The optimal set of policy parameter θ^*
Optimize $\mathcal{L}$ w.r.t. policy parameter θ using $\mathcal{D}^E$

Model-Free methods learn a policy that reproduces the expert's behavior without learning/estimating system dynamic. Since they do not require neither to estimate the dynamic nor to learn a reward function, they are simple to implement and do not necessary require interactions with the environment during the learning procedure.

Model-Free methods that derive policy in the trajectory space were very popular in the context of Model-Free BC for trajectory planning, given their ability to explicitly model constraints (e.g. a smooth convergence to the goal state). In this setting well studied methods are the *Dynamic Movement Primitives* (DMPs) [33, 34], which can represent non-linear movements without losing the stability of the behavior. Authors in [34] formulated the Dynamic Movement Primitive for a single DoF point-to-point trajectory using the following set of non-linear differential equations:

$$\tau \dot{y} = \beta_s(\alpha_s(g - s) - y) + f(z) \tag{1.1}$$

$$\tau \dot{s} = y \tag{1.2}$$

$$\tau \dot{z} = -\alpha_z z,\ z(t) = z_0\ exp(-\frac{\alpha_z}{\tau}t) \tag{1.3}$$

Where $\beta_s, \alpha_s, \alpha_z$ are constants, s is the system state, z is the phase-variable function of time t, and f is the forcing-term which describes the trajectory non-linear behavior. Generally, f is a linear combination of basis-function $\psi_i(z)$ (e.g., Gaussian basis function), $f(z(t)) = (g - s_0)\sum_{i=1}^{M} \psi_i(z(t))\omega_i z$. Basically, a DMP describes a point-attractor system, where the current system state s must converge to the goal state g, starting from s_0. In this setting, the aim is to learn the set of weights, $\{\omega_i, i = 1, \ldots, M\}$, which can be obtained by solving a supervised learning problem with loss function $\mathcal{L}_{DMP} = \sum_{t=0}^{T}(f_{target}(t) - f(z(t)))^2$, where $f_{target}(t) = \tau^2\ \ddot{s}^E - \beta_s(\alpha_s(g - s^E) - \tau\dot{s}^E)$. DMPs formulation has been used in the context of robotic manipulation. For example in [35, 36, 37] the problem of task decomposition was faced, and DMPs have been used to model the sub-tasks. However, DMPs formulation has a series of problems related to: (**a**) how to handle stochasticity in demonstrations; (**b**) how to explicitly define basis function, given the desired behavior; (**c**) how to handle arbitrary desired trajectories, with intermediate via-points; (**d**) how to handle complex high-dimensional inputs. For all the above mentioned problems some solutions have been proposed. For example, the stochasticity problem was addressed in [38], where the Probabilistic Movement Primitives (ProMPs) method was proposed. In ProMPs the probability of observing a trajectory $\boldsymbol{\tau}$ is written as $\boldsymbol{\tau} = \prod_t \mathcal{N}(s(t)|\Psi(z(t))^T\omega, \Sigma_s)$, where Ψ is a time-dependent basis matrix. As in DPMs, the goal is to find the weights ω, by solving a supervised learning problem. As for the second problem, other trajectory representations have been proposed based on Hidden

Markov Model, Gaussian Mixture Models, Kernelized Movement Primitives. However, all these alternatives scale bad when the goal is to learn a policy starting from visual observations. To handle such complex high-dimensional input Deep Architecture have been proposed, which will be explained in detail in the next sections.
Regarding the methods that derive the policy in the action-space. One of the primal work was [39], which proposed *ALVINN*, an autonomous vehicle driving system based on a Neural Network, that infers the steering angle, given a synthetic camera image as input. The network was trained on pairs (image, steering-angle) and the training procedure was defined as a supervised classification problem, since the steering-angle was discretized over 45 units. This work immediately emphasized the problem of compounding-error, caused by **covariate-shift phenomena**. This issue occurs because an action a_t influences the next state s_{t+1}, which represents the next sample, violating the i.i.d assumption of Supervised Learning and generating a test-data distribution, that may be different from the training one. This phenomena has a relevant consequence on the expected performance of the system. Indeed, assuming to have a system that makes an error with probability ϵ, and a task with time-horizon T, then, due to compounding error, a supervised learner reaches a total cost of $O(\epsilon\, T^2)$, rather than $O(\epsilon\, T)$ [40, 41]. To attenuate this problem, interactive supervised learning algorithms have been proposed, such as the well-known *DAgger* [41]. Algorithm 2 describes the DAgger procedure. It is an aggregation strategy, based on the idea to train the policy π^L under the state-distribution induced by the policy itself, but with the correct action performed by the expert. The main problem with DAgger is that it requires the expert to interact with the system during the training, introducing both safety and data-efficiency problems, especially when the system does not provide the human expert with sufficient control authority during the sampling process [42].

Algorithm 2 DAgger Algorithm [41]

Require: Initial Dataset $\mathcal{D} \leftarrow \emptyset$, Initial policy π_1^L
Ensure: The best policy π_i^L
  for $i = 1, \dots N$ **do**
    Sample $T - step$ trajectories using π_i^L
    Let $\mathcal{D}_i = (s_t, \pi^E(s_t))$, state s_t visited by policy π_i^L, and actions given by the expert
    Aggregate Dataset, $\mathcal{D} \leftarrow \mathcal{D} \bigcup \mathcal{D}_i$
    Train policy π_i^L on $\mathcal{D}$
    Let $\pi_{i+1}^L = \beta_i \pi^E + (1 - \beta_i)\pi_i^L$
  end for

Human-Guided DAgger (HG-DAgger) [43] is an extension of the classic DAgger strategy, in which the human expert observes the rollout of the current policy, so if the agent has entered an unsafe region of the state space, the expert takes control and guides the system to a safe and stable region. In [5] was shown how HG-DAgger can be effectively used in the context of robotic manipulation. Indeed, starting from the same total number of episodes, a policy trained with only expert demonstration has a significantly lower success rate than a policy trained on a dataset with both expert demonstrations and expert adjustments. In the context of Interactive Learning for Robot Manipulation, other works of interest include [44, 45]. In [45], a human expert provides both **corrective** and **evaluative** feedback. The former consists in the human that takes control of the robot to adjust the trajectory, the latter consists in a scalar weight q, set to 1 if the trajectory is satisfactory, 0 if the trajectory is not satisfactory, α if the trajectory is adjusted by

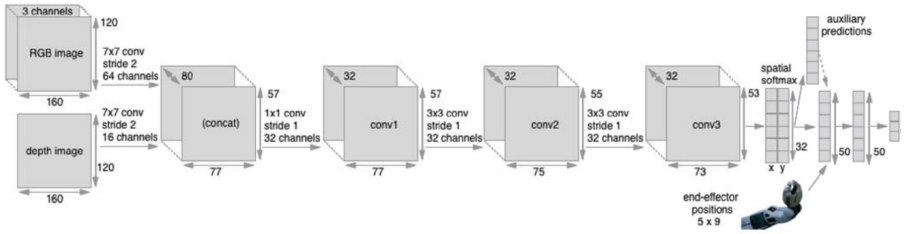

Figure 1.6: Architecture proposed in [20]

Table 1.1: Statistics of Training set, and Test Success rate [20]

task	reaching	grasping	pushing	plane	cube	nail	grasp-and-place	grasp-drop-push	grasp-place-x2	cloth
#demo	200	180	175	319	206	215	109	100	60	100
demo duration (min)	13.7	11.1	16.9	25.0	12.7	13.6	12.3	14.5	11.6	10.1
Test success rate (%)	91.6	97.2	98.9	87.5	85.7	87.5	96.0	83.3	80.0	97.4

the expert, where α is the ratio between non-corrected and corrected samples. Then a Neural Network was trained by minimizing a weighted version of the maximum-likelihood, $\mathcal{L}(a_t, s_t) = -q\ log(\pi_\theta^L(a_t|s_t))$. Real-world experiments show that with a training time of **41 minutes**, including environmental reset, it was possible to have an agent capable of performing tasks such as picking up a cube or pulling a plug.

Despite the covariate-shift problem, [20] showed that very interesting performance can be obtained in the context of Robot Manipulation, by means of Behavioral Cloning and high quality demonstrations given by teleportation system. In this work, a Convolutional Neural Network was trained to predict the desired linear-velocity, angular-velocity of the end-effector, and the binary gripper state (open/close), given in input the current RGB-D observation of the scene, and the position of three points of the end-effector, during the last 5 time-steps (Figure 1.6). The system was tested on 10 tasks, and the performance are reported in Table 1.1. The proposed system achieved a high success rate while evaluating all the tasks. The tests were carried out from different initial conditions but still quite similar to those present in the training set (e.g., the initial object positions have been uniformly distributed within the training regime, with random local variations around these positions). The analysis of failure cases showed that the leading cause of errors was the inability to detect critical points in the task execution, such as closing/opening the gripper to pick/place the object or detect the position of the object of interest in order to avoid collision with it. Another important aspect to note is that, for each task, the network was trained from scratch. This is not a desired property for a highly adaptable system, as stated in Section 1.1. For this reason, methods based on Meta-Learning algorithms have been proposed.

The idea behind Meta-Learning is to train a model on a variety of tasks, in such a way that it can solve a new task, using only a small number of training samples [46]. Algorithm 3 describes the steps followed by the *Model-Agnostic Meta-Learning* (MAML) algorithm [46], that is the base for different methods which apply One-shot Imitation Learning in the context of Behavioral Cloning [47, 48, 49].

In [47], MAML algorithm was used to prove the effectiveness of Meta-Learning in the context of real robot manipulation, with visual observations, as opposite to [50]. A Convolutional Neural Network was trained by following the Algorithm 3, using as loss-function the Mean Squared Error, computed between the predicted action and the ground truth

Algorithm 3 Model-Agnostic Meta-Learning (MAML) [46]

Require: Distribution over tasks $p(\mathcal{T})$
  Randomly initialize θ
  while $i = 1, \dots N$ **do**
    Sample batch of tasks $\mathcal{T}_i \sim p(\mathcal{T})$
    for all $\mathcal{T}_i$ **do**
      Evaluate $\nabla_\theta \mathcal{L}_{\mathcal{T}_i}(f_\theta)$ w.r.t. K examples
      Compute adapted parameters with gradient descent: $\theta_i' = \theta - \alpha \nabla_\theta \mathcal{L}_{\mathcal{T}_i}(f_\theta)$
    end for
    Update $\theta \leftarrow \theta - \beta \nabla_\theta \sum_{\mathcal{T}_i \sim p(\mathcal{T})} \mathcal{L}_{\mathcal{T}_i}(f_{\theta_i'})$
  end while

one. For real-robot experiments a dataset of **1300** placing demonstrations (i.e., place an holded object in a target container), containing near to **100** different objects, was collected through teleportation. The trained system was tested by performing the adaptation step on one video demonstration, over 29 new objects, moreover, between the video demonstration and the actual execution, the objects configuration was changed. In this setting the system reached the **90**% of success rate, outperforming baseline methods based on LSTM [50], and contextual network (i.e., a Convolutional Neural Network that takes in input the current observation and the image representing the target state). In [48], the *Domain Adaptive Meta-Learning* algorithm (DAML) was proposed with the goal of learning to infer a policy from a single human demonstration. To achieve it, a two-step algorithm was proposed. In the first-step, called **Meta-Learning step**, given in input, for each task $\mathcal{T}$, a set of human demo $\mathcal{D}_\mathcal{T}^h$ and a set or robot demo $\mathcal{D}_\mathcal{T}^r$ (Figure 1.7), the *initial policy parameters* θ and the *adaptive loss* parameters ψ are learned, solving the problem in Formula 1.4.

$$\min_{\theta,\psi} \sum_{\mathcal{T} \sim p(\mathcal{T})} \sum_{\mathbf{d}^h \sim D_\mathcal{T}^h} \sum_{\mathbf{d}^r \sim D_\mathcal{T}^r} \mathcal{L}_{BC}(\theta - \alpha \nabla_\theta \mathcal{L}_\psi(\theta, \mathbf{d}^h), \mathbf{d}^r) \tag{1.4}$$

Where the outer loss is $\mathcal{L}_{BC}(\phi, \mathbf{d^r}) = \sum_t log(\pi_\phi(a_t|s_t, o_t))$, and the inner-loss $\mathcal{L}_\psi$, is the learned adaptive loss, which is used during the **Meta-Test step**, where the policy parameters are adapted with gradient descent given in input a video of human demonstrating a new task $\mathcal{T}$, i.e., $\phi_\mathcal{T} = \theta - \alpha \nabla_\theta \mathcal{L}_\psi(\theta, \mathbf{d}^h)$. Experimental evaluation on tasks such as placing, pushing, and pick-and-place, has shown that: **(a)** the system was able to generalize across both new objects and objects configuration starting from only a single human-demonstration; **(b)** a performance degradation was observed in large domain-shift experiments, such as novel backgrounds and different camera view-points.

All the works described up to now, consider the task distribution $p(\mathcal{T})$ as composed of one-single task, but with many different variations [47] or different, but related tasks [48]. Very recent methods try to generalize BC to a huge variety of tasks [5, 4]. In [5], a large-scale dataset containing **100** diverse manipulation tasks was collected. The demonstrations were collected through both expert teleoperation and shared autonomy process (HG-DAgger [43]). The demonstrated tasks were related to pick-and-place, grasp, pick-and-drag, pick-and-wipe, and push skills. The dataset was used to train the network in Figure 1.8. As it can be noted the samples were composed by the current robot observation, and a conditioning represented by either a natural language description or a human video demonstration. The idea was that training a conditioned policy over the current ob-

Figure 1.7: Tasks performed in [48]. (Top row) Human demonstration, (Bottom row) robot demonstration. (Left) Placing task, (Middle) pushing task, (Right) pick-and-place task.

servation o_t, and a task representation c, $\pi^L(a_t|o_t, c)$, it would allow the policy to generalize over new tasks in a zero-shot manner (i.e., without any fine-tuning). Experimental results shown that, over 28 held-out tasks, containing both completely new objects, and known objects but in different tasks, an average success rate of **38%** was reached in the easiest setting, with only one distractor and with natural language instruction. The success rate dropped to **4%** in the hardest setting with 4 distractors and video conditioning. In their analysis, the authors pointed out that the system did not fail to identify the object, but in what they called "**last-centimeter errors**", i.e., failing to close the gripper, failing to let go of objects, or a near miss of the target object when letting go of an object in the gripper. Authors in [4] did a further step towards Multi-task Imitation Learning. They proposed Multi-task One-Shot imitation with self-AttentIon and Contrastive Learning (MOSAIC), an architecture designed to model a demonstration-conditioned policy, $\pi_\theta^L(a_t|o_t, d)$ where d is the current task demonstration (e.g., a video of a robot performing the task), and solve the multi-task imitation learning problem by incorporating two key components: **(1)** a time-contrastive loss as additional supervision for representation learning, with the aim to obtain similar embeddings for temporally close-by frames; **(2)** a self-attention model architecture with the aim to extract contextual information from demonstrations, used by the Neural Network to infers the action. A dataset with 7 different tasks and 61 variations was collected by running hand-written policies in a simulation environment. It was used to train and compare the proposed architecture against other one-shot imitation learning methods [48, 51]. The results in Table 1.2 show that MOSAIC outperformed previous methods in the Single-Task One-shot Imitation Learning Setting, i.e., one-task with multiple variations and tested on unseen variations. Moreover, when tested in a Multi-Task setting, i.e., training the system on all the tasks and testing it on each task separately, the system partially replicates the demonstrated task. In general, transitioning from a single-task to a multi-task setting is not trivial. Indeed, the success rate decreases for almost all

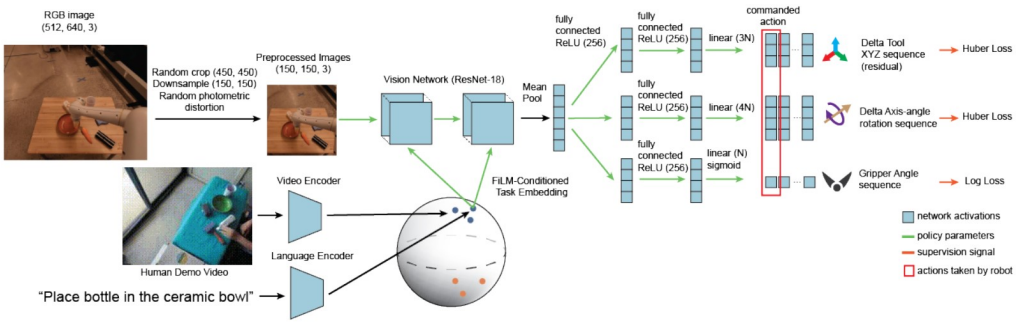

Figure 1.8: Architecture proposed in [5]

Table 1.2: Results obtained in single-task and multi-task one-shot imitation learning [4].

Task	Setup	DAML [48]	T-OSIL [51]	MOSAIC [4]
Open door	single	23.3 ± 5.2	57.9 ± 7.1	**67.1 ± 5.5**
	multi	10.8 ± 5.4	49.2 ± 6.0	**68.3 ± 6.3**
Open drawer	single	15.4 ± 5.5	57.5 ± 3.9	**65.4 ± 3.4**
	multi	3.3 ± 1.4	53.3 ± 4.0	**55.8 ± 3.6**
Press button	single	62.8 ± 3.9	56.4 ± 2.4	**71.7 ± 3.9**
	multi	1.7 ± 0.7	63.3 ± 3.5	**69.4 ± 3.4**
Pick-and-Place	single	0.0 ± 0.0	74.4 ± 2.1	**88.5 ± 1.1**
	multi	0.0 ± 0.0	19.5 ± 0.4	**42.1 ± 2.3**
Stack block	single	10.0 ± 1.8	13.3 ± 2.6	**79.3 ± 1.8**
	multi	0.0 ± 0.0	34.4 ± 3.4	**70.6 ± 2.4**
Basketball	single	0.4 ± 0.3	12.5 ± 1.6	**67.5 ± 2.7**
	multi	0.0 ± 0.0	6.9 ± 1.3	**49.7 ± 2.2**
Nut assembly	single	2.2± 1.4	6.3 ± 1.9	**55.2 ± 2.8**
	multi	0.0 ± 0.0	6.3 ± 1.3	**30.7 ± 2.5**

the tasks, even though the tasks are known (i.e., used during the training). It indicates the need to have both training procedures and architectures capable of extrapolating embeddings that are representative of both the task itself and the different sub-tasks, in order to reuse them when executing a new instance or a completely new task. The results reported by the different methods pointed out how there is a wide room for improvement in the context of both Single-Task and Multi-Task Few-shot Imitation Learning methods, which are particularly promising when it comes to task-level generalization, because the intent of the new task is correctly captured, especially in the case of conditioned policies. However, the success rate in task execution is relatively low for several reasons that can range from difficulty in identifying key points in task execution (e.g., the robot has approached the object and, therefore, the gripper must be closed) to compounding error, which leads to new observations different from those in the training set (e.g., the robot did not grasp the object correctly). As a result, the robot cannot complete the task because it performs actions inconsistent with the state of the task itself. Possible improvements can range from using a multi-modal system based on visual and tactile information in order to make explicit the transition between consecutive task phases, to adding bad demonstrations combined with recovery behavior during data collection.

The methods presented up to now partially solve the problems related to compounding error and task-generalization. Another relevant problem related to Behavioral Cloning, and more in general to Learning from Demonstration, is the execution of **multi-stage long-horizon tasks**. Indeed, it is pretty intuitive to think that a manipulation task is characterized by a modular structure which can be exploited to improve performance, following the idea that each sub-task can be learned more efficiently because each skill is shorter-horizon. In this setting, the main question to answer is: *How can a task be decomposed into the corresponding component skills?* In its classical formulation, this problem can be framed as a classification problem. In a preliminary work [35], the authors used a set of predefined primitive motions modeled as DMPs. The goal was to recognize these primitives within the demonstrated trajectory using an Expectation-Maximization algorithm. Also, recent methods [36, 37] exploit the DMPs formulation. However, they are not part of the process of task segmentation. For example, in [36], the action segmentation is performed based on either object proximity or explicit human command. When the robot manager identifies a new action, the corresponding DMP is learned, and the sequence of

tasks is organized in a hierarchical structure. The problem of task-segmentation was also solved starting from an unconstrained video demonstrations labeled with commands [52], activity [53], or completely unlabeled [49, 54]. In [49], the authors proposed an extension of DAML for multi-stage tasks. The main idea of this work was based on modeling the distribution of tasks, $p(\mathcal{T})$ as a set of primitives (e.g., reach primitive). During the meta-training phase, two systems were obtained: (**1**) a human/robot-phase predictor, whose responsibility was to indicate the completion rate of the current primitive given a human video demonstration and a robot video demonstration, respectively; (**2**) a Convolutional Neural Network trained according to DAML, which acted as a motion-primitive meta–model policy, parameterized by meta-parameters θ. During the meta-test phase, given as input a video of human performing a compound task, three steps were defined: (**1**) extrapolate the set of primitives by using the human-phase predictors; (**2**) for each primitive, starting from the meta-parameters θ, find the parameters ϕ_i by performing gradient descent on the learned loss function $\mathcal{L}_\psi$; (**3**) execute the policy parameterized by ϕ_i, until the current sub-task is completed (completion detected by the robot-phase predictor). The work proposed in [54] addressed the multi-stage long-horizon tasks with a different approach. The authors did not focus on an explicit concept of task segmentation. Indeed, they started with the idea that similar tasks intersect at common regions of the state-space, and proposed a two-stage IL architecture able to exploit this intersecting structure to generalize to unseen start-goal state combinations.
These methods are interesting because they allow the execution of a compound task from simple unlabeled videos, thus with as little effort as possible in dataset generation. However, since they do not have semantic information about which part of the task is being executed, they may err on the side of interpretability of actions, which is not the case with methods based on labeled videos or hierarchical structures.

Model-Based methods are characterized by the fact that during the learning process the system dynamic model is learned. There are several reasons why it may be necessary to use the dynamic system model in the context of Learning from Demonstration, for example: **(a)** a difference in the embodiment between the demonstrator and the learner; **(b)** a difference in the task execution conditions and parameters. Among these methods, the most important aspect is related to how the dynamic model is retrieved, e.g., Gaussian Mixture Model [55] or Gaussian Process [56, 57]. In recent years, a significant amount of attention has been placed on systems that can replicate a task from a video of human performing a task without any access to ground-truth action. While in the survey mentioned before, these methods were still considered Model-Based Behavioral Cloning. In the current literature, given the increasing amount of works, they can now belong to a new category called Learning from Observation. Methods belonging to this category will be explained in the specific paragraph.

Inverse Reinforcement Learning (IRL)
Inverse Reinforcement Learning or Inverse Optimal Control is a Learning from Demonstration approach that was introduced in [58]. In IRL, starting from a set of expert-demonstrated trajectories, the main goal is to obtain the *Reward function* R, which explains the expert behavior. Once R is found, an RL algorithm is run to obtain the policy π_θ^L (Algorithm 4). An important design choice is related to how parametrize the reward-function, i.e., a **linear** function of the features [59, 60] or a **non-linear** function of the features [61, 62, 63]. Generally, the IRL algorithms are characterized by the following problems: **(1)** the learning process could be time-consuming and impractical for high-di-

Algorithm 4 Classic feature matching IRL algorithm

Require: Dataset of expert trajectories $\mathcal{D} = \left\{\boldsymbol{\tau}_i^E\right\}_{i=1}^N$
Require: Reward function R_ω, policy π_θ^L
  while policy improves **do**
    Evaluate the state-action visitation frequency μ of the current policy π_θ^L
    Evaluate the objective function $\mathcal{L}$, w.r.t. μ and the dataset $\mathcal{D}$
    Update the reward-function parameters ω based on $\mathcal{L}$
    Update the policy π_θ^L through an RL algorithm, using the updated R_ω
  end while

mensional problems, because of the double-nested optimization procedure; **(2)** the IRL problem is *ill-posed*, since there are different reward-functions that could lead to the same action.
Some constraints to the optimization procedure have to be added to solve the problem of multiple solutions. Based on the constraint type, the two main IRL procedures can be identified, which are: **(a)** The *Maximum Margin Prediction* (MMP) approach [59, 61]; **(b)** *Maximum Entropy* (Max-Ent) approach [60, 62, 63]. The MMP methods assume that the demonstrated trajectories are optimal and work in a deterministic setting. The aim is to find the cost-function such that the reward of the demonstrated trajectories, $R(\boldsymbol{\tau}^E)$, is greater than the reward of all the alternative trajectories, $R_\omega(\boldsymbol{\tau})$, by a certain margin m, i.e., $\max_{\omega,m} m \;\; s.t. \; R_\omega(\boldsymbol{\tau}^E) \geq \max(R_\omega(\boldsymbol{\tau})) + m$. The main problem with this formulation is that it does not handle the case in which the expert behavior is sub-optimal, leading to an ambiguous notion of margin. To handle this problem the Max-Ent approach has been proposed in [60]. In Max-Ent the goal is to find the reward-function parameters ψ that drives the policy to maximize the entropy, subject to the feature expectation matching, i.e $\max_{\psi} \mathcal{H}(\pi^{r_\psi}) \; s.t. \;\; \mathbb{E}_{\pi^{r_\psi}}[\mathbf{f}] = \mathbb{E}_{\pi^*}[\mathbf{f}]$. The setting based on the Maximum Entropy is the most popular in the IRL field since it removes the ambiguous aspects of the previous formulation. In the original work, the reward-function was a linear combination of the features, i.e., $r_\psi = \psi^T \mathbf{f}$. However, this reward formulation is not suited for high-dimensional feature space, which can require the capability to model non-linear reward structures. In [62], a deep-network was used to model the reward-function. In this work, the Nerual Network maps the feature vector $\mathbf{f}$ into the reward value, and trained according to the Maximum-Entropy setting. Experimental results have shown that the ability to approximate highly non-linear reward functions is essentially to successfully solve tasks in high-dimensional discrete state space. A generalization to continuous state space was proposed in [63]. In particular, [63] faced the problem of learning a cost function in a high-dimensional continuous state space, with **unknown dynamics**. Indeed, starting from the exponential trajectory distribution $p(\tau) = \frac{1}{Z}\, exp(-c_\theta(\tau))$, the main difficulty is the estimation of the partition function Z, needed to compute the negative log-likelihood loss function, $\mathcal{L}_\theta = \frac{1}{N} \sum_{\tau_i^E \in D_{demo}} c_\theta(\tau_i^E) + \log(Z)$. Since, the dynamic is unknown the idea was to estimate the partition function through the trajectories obtained from the current policy rollouts, with the hyphothesis that, during the learning of the cost function, the current policy drives the distribution towards regions where samples are more useful. Starting from these considerations, the Algorithm 5 was proposed. The algorithm [64] returns a *Linear-Quadratic Gaussian* controller q_k, such that

Algorithm 5 Guided-Cost-Learning Algorithm [63]

Require: Initial controller $q_k(\tau)$
  for i = 1, ..., N **do**
    Generate D_{traj} from $q_k(\tau)$
    $\mathcal{D}_{samp} \leftarrow \mathcal{D}_{samp} \bigcup \mathcal{D}_{traj}$
    Update the cost-function parameters, using $\mathcal{D}_{samp}$ and $\nabla_\theta \mathcal{L}(\theta)$
    Update the controller $q_{k+1}(\tau) \leftarrow q_k(\tau)$ according to [64] and using $\mathcal{D}_{traj}$
  end for

$q_k = \underset{q}{argmin}\ \mathbb{E}[c_\theta(\tau)] - \mathcal{H}(\tau)\ s.t.\ p(s_{t+1}|s_t, a_t) = \mathcal{N}(s_{t+1}; f_{x_t}x_t + f_{u_t}u_t, F_t)$. The cost-function was parameterized according to a Neural Network, and experiments performed on real-robot manipulation tasks such as dish placement and pouring proved the effectiveness of the proposed method and the need to have a non-linear representation of the cost function for complex problems, outperforming the classic Max-Ent method. Recent method [65] tried to move IRL towards more complex learning scenario, such as learning a reward function from video-demonstrations. In [65] the architecture in Figure 1.9 was proposed. The goal was to obtain the parameters Ψ, of a cost function $C_\Psi(\hat{\boldsymbol{\tau}}, z_{goal})$, such that it was possible to derive a sequence of actions by minimizing the cost-function itself, i.e., $\mathbf{a}_{new} = \mathbf{a} - \eta \nabla_a C_\Psi(\hat{\boldsymbol{\tau}}, z_{goal})$, Different cost functions have been proposed, but all with the same objective to reduce the distance between the current predicted keypoints and the goal keypoints configuration. The trajectory $\hat{\boldsymbol{\tau}}$ is a a sequence of predicted states $[\hat{s}_1, \ldots, \hat{s}_T]$, result of a learned dynamic model, $\hat{s}_{t+1} = f_{dyn}(\hat{s}_t, a_t)$. Experimental results have shown that it is possible to learn a cost-function starting from human/robot video demonstrations. However, the proposed setting was tested on a very simple reaching task, proving how a lot of work has to be made in order to prove the effectiveness or ineffectiveness of IRL in complex real-robot manipulation tasks, starting from video demonstrations.

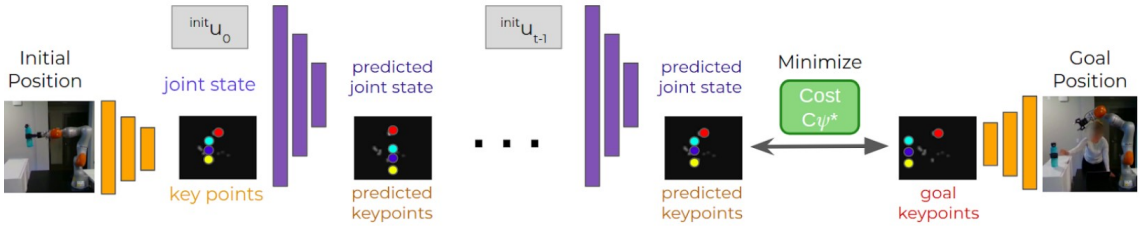

Figure 1.9: Architecture proposed in [65]

Generative Adversarial Imitation Learning (GAIL)

Generative Adversarial Imitation Learning was proposed for the first time in [66], with the idea to improve the IRL setting, which is expensive to run, because of the double-nested optimization procedure. The authors in [66], starting from a general Max-Ent formulation (Formula 1.5), obtained a characterization of the learned policy (Formula 1.6), where $\psi(c)$ is a cost-regularizer, $\psi^*(c)$ is its conjugate, and ρ_π is the occupancy measure, i.e., the distribution of state-action pairs that the agent encounters when navigating the environment with policy π. The interpretation of Formula 1.6 is that the $\psi - regularized$ IRL finds a policy whose occupancy measure is similar to the expert's one, measured by

Algorithm 6 Generative Adversarial Imitation Learning Algorithm

Require: Expert Trajectories $\tau^E \sim \pi^E$, initial policy π_θ^L, discriminator D_ω
  for $i = 1, \ldots, N$ **do**
    Sample trajectories, $\tau_i^L \sim \pi_\theta^L$
    Update Discriminator, $\hat{\mathbb{E}}_{\tau_i^L}\left[\nabla_\omega \log(D_\omega(s,a))\right] + \hat{\mathbb{E}}_{\tau^E}\left[\nabla_\omega \log(1 - D_\omega(s,a))\right]$
    Update Policy π_θ, with TRPO [70], and cost-function $C(s,a) = \log(D_\omega(s,a))$
  end for

ψ^*. The next-step was to choose an appropriate regularization function. In particular, by choosing the regularizer in Formula 1.7, the conjugate in Formula 1.8 can be obtained, which is the classic Adversarial-Learning Loss, where the current policy π^L plays the role of GAN generator, and D is the GAN discriminator, which has to distinguish between state-action pairs generated either by the expert-policy or by the current policy.

$$IRL_\psi(\pi^E) = \underset{c \in R^{S \times A}}{arg\ max} - \psi(c) + (\min_{\pi^L \in \Pi} - \mathcal{H}(\pi^L) + \mathbb{E}_{\pi^L}\left[c(s,a)\right]) - \mathbb{E}_{\pi^E}\left[c(s,a)\right] \tag{1.5}$$

$$RL \circ IRL_\psi(\pi^E) = \underset{\pi^L \in \Pi}{arg\ min} - \mathcal{H}(\pi^L) + \psi^*(\rho_{\pi^L} - \rho_{\pi^E}) \tag{1.6}$$

$$\psi_{GA}(c) = \begin{cases} \mathbb{E}_{\pi^E}\left[g(c(s,a))\right] & if\ c < 0 \\ +\infty & otherwise \end{cases}, \; g(x) = \begin{cases} -x - log(1 - e^x) & if\ c < 0 \\ +\infty & otherwise \end{cases} \tag{1.7}$$

$$\psi^*_{GA}(\rho_{\pi^L} - \rho_{\pi^E}) = \max_{D \in (0,1)^{S \times A}} \mathbb{E}_{\pi^L}\left[\log(D(s,a))\right] + \mathbb{E}_{\pi^E}\left[\log(1 - D(s,a))\right] \tag{1.8}$$

Based on these considerations the Algorithm 6 has been proposed. The algorithm comprises two fundamental steps, the first related to the Discriminator's parameter update and the second related to the policy's parameter update. Since GAIL has proven to be more effective than classic IRL algorithm [60], subsequent works have focused either on improving the sample efficiency, by replacing the model-free on-policy TRPO algorithm, with an off-policy RL algorithm, such as in [67], or by modifying the reward function in input to the RL algorithm [68, 69]. All the cited methods have reported promising results on control tasks in a simulation environment [71], but they worked in a low-dimensional state-space, indeed when the GAIL method was adapted to work with a high-dimensional state-space, like in [72, 73, 74, 75], it shown very poor results. In particular, with respect to the Adversarial Imitation Learning setting, works of interest are [74, 75]. In [74], the authors focused on solving the **casual-confusion** problem. This problem occurs when the discriminator, during the learning process, focuses on task-irrelevant features between expert and policy generated transitions, this causes the rewards to become uninformative. To reduce the casual-confusion problem, in [74] two elements have been proposed: (**1**) a regularization term, with the aim to make the discriminator **unable** to distinguish between constraining sets I_E and I_A. These sets are composed of expert and agent observations, such that a sample can belong either to I_E or I_A, based on spurious features (e.g., a different gripper color); (**2**) an early-stopping policy called Actor Early-Stopping (AES), that restarts the episode if the discriminator score at the current step exceeds the median score of the episode so far for $T_{patience}$ consecutive steps. The regularization term was

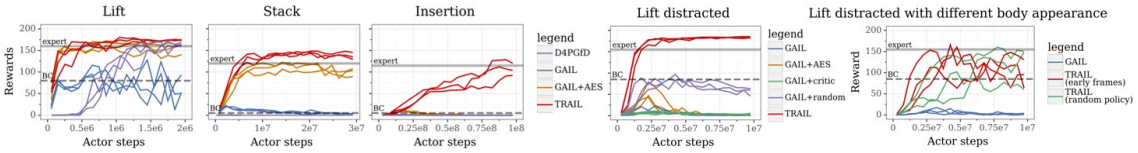

Figure 1.10: Experimental results on tasks without and with spurious features [74]

defined as $accuracy(\mathcal{I}_E, \mathcal{I}_A) = \frac{1}{2}\ \mathbb{E}_{s\in\mathcal{I}_E}\left[\mathbf{1}_{D_\omega \geq \frac{1}{2}}\right] + \frac{1}{2}\ \mathbb{E}_{s\in\mathcal{I}_A}\left[\mathbf{1}_{D_\omega < \frac{1}{2}}\right]$. In the end, the discriminator's parameters were the result of $\max_{\omega} G_\omega(s_E, s_A) - \mathbf{1}_{accuracy(\hat{s}_E, \hat{s}_A) \geq \frac{1}{2}} G_\omega(\hat{s}_E, \hat{s}_A)$, where G_ω is the discriminator binary cross-entropy, $\hat{s}_E \in \mathcal{I}_E$, and $\hat{s}_A \in \mathcal{I}_A$. An agent was trained on each single task, according to the Distributed Distributional Deterministic Policy Gradients (D4PG) [76] RL algorithm, with reward-function $R(s_t) = -\log(1 - D_\omega(s_t))$. Experimental results have shown how the proposed system overcomes the GAIL [66] baseline, both in setting with spurious features and without spurious features (Figure 1.10).

The authors of [75] made a step towards a more data efficient Adversarial Imitation Learning method. Indeed, they leveraged the idea of using a model-based approach in the context of high-dimensional state space. Still, instead of generating a dynamic model in the image space, the proposed method is based on encoding the observations defined in the image space into a corresponding latent space characterized by vectors of smaller dimension. Then subsequently go on to learn a dynamic model in that space. In this context the learning procedure is based on three main steps: **(1)** learn the *Latent Dynamic Model*, $(\hat{\mathcal{U}}_\beta, \hat{\mathcal{T}}_\beta, q_{beta})$, by maximizing the Evidence Lower Bound (Formula 1.9), where $\hat{\mathcal{U}}_\beta$ is the decoder, q_{beta} is the encoder, and $\hat{\mathcal{T}}_\beta$ is the transition model; **(2)** train a *discriminator*, D_θ, by minimizing the Adversarial Loss function (Formula 1.10); **(3)** train a *policy* π_θ^L, by maximizing the Value function (Formula 1.11).

$$\max_{\beta}\ \mathbb{E}_{q_\beta}\left[\sum_t \log(\hat{\mathcal{U}}_\beta(s_t|z_t)) + \mathbb{D}_{KL}(q_\beta(z_t|s_t, z_{t-1}, a_{t-1})||\hat{\mathcal{T}}_\beta(z_t|z_{t-1}, a_{t-1}))\right] \tag{1.9}$$

$$\min_{\theta}\ \mathbb{E}_{(z,a)\sim\rho^E(z,a)}\left[-log(D_\theta(z,a))\right] + \mathbb{E}_{(z,a)\sim\rho^{\pi^L}_{\hat{\mathcal{T}}}}\left[-\log(1 - D_\theta(z,a))\right] \tag{1.10}$$

$$\max_{\pi_\theta^L}\ V^K_{\theta,\beta}(z_t) = \max_{\pi_\theta^L}\ \mathbb{E}_{\pi_\theta^L, \hat{\mathcal{T}}_\beta}\left[\sum_{\tau=t}^{t+K-1} \gamma^{\tau-t} \log(D_\theta(z_\tau^{\pi_\theta^L}, a_\tau^{\pi_\theta^L})) + \gamma^K V_\beta(z_{t+K}^{\pi_\theta^L})\right] \tag{1.11}$$

With this learning setting the proposed system outperforms previous works such as [73, 67] both in terms of data-efficiency and overall performance, on a set of control tasks (Figure 1.11). Generally speaking, the Generative Adversarial Imitation Learning has shown very promising performance in simulated control tasks and simulated robot manipulation tasks, even in complex high-dimensional state-space. However, it is not so clear, how these methods could perform in real-world robotic manipulation tasks, in terms of data-efficiency, generalization capability, and safety during real-world interactions.

Learning from Observation (LfO)

The goal of *Learning from Observation* is to learn a policy by leveraging **state-only-demonstration**. This approach has gained attention in recent years because it theoretically allows a robotic system to be programmed as naturally as possible. In fact, in the

Figure 1.11: Control tasks solved in [75]. From left to right: cheetah run, walker walk, car racing, claw rotate, baoding balls

most promising setting, a robotic system should be able to reproduce a task by observing a human or another robot performing it, without having access to the action performed, as is the case in all the methods described so far. In designing a LfO system there are at least three aspects to consider: **(1)** in the case the demonstrator has a different embodiment with respect to the imitator, how can the embodiment mismatch be solved?; **(2)** in the case the demonstrator viewpoint differs from the imitator one, how can the correspondence problem between the two different viewpoints be handled?; **(3)** once the problems related to the perception subsystem are solved, how is the policy π^L obtained?.

First of all, the points **(1)** and **(2)** are going to be answered. Regarding, the embodiment mismatch, this may happen, for example, when the video demonstration shows a human performing a task, but the goal is to train a robot (Figure 1.12). To solve this problem, in [29, 77, 78], some sort of image-to-image translation was performed, while in [79] the *Temporal-Cycle Consistency* (TCC) [80] was used.
In particular, in [29, 78], the Cycle-GAN [81] was used to translate image from the source domain (human image) into the corresponding target domain (robot image). The need for an unsupervised image-to-image translation architecture such as the Cycle-GAN arises from the fact that there are not paired images. The network learns two mappings, the first from the source to the target domain $G : X \rightarrow Y$, the second from the target to the source domain $F : Y \rightarrow X$. The dataset for the source domain was composed of human demonstrations as well as a small amount of "random" data, in which the human moves around the scene but does not specifically attempt the task, while for the target domain, it consists of robot images executing randomly sampled actions in a few different settings. In [77] a similar approach was proposed, but the MUNIT [82] architecture was adopted for the image-to-image translation. With respect to the mentioned works, in [79] a completely different approach has been proposed. Indeed, starting from a set of video demonstrations characterized by both different length and demonstrator embodiment, the TCC approach was used to learn an encoder able to map demonstration frame into the corresponding embodiment-independent embedding. The idea behind TCC was to learn

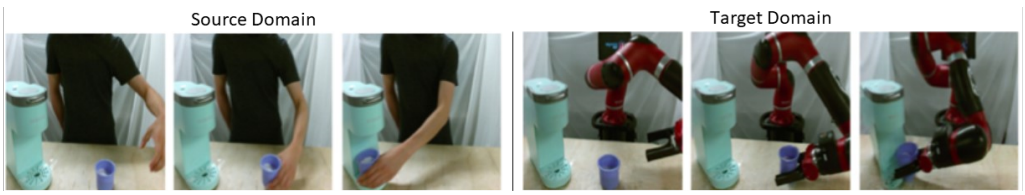

Figure 1.12: Representation of embodiment mismatch problem. (Left) The source domain represented by a video of human performing a task. (Right) The target domain, represented by the robot that executes the observed task.

a correspondence between frames of different videos representing the same overall action (Figure 1.13).

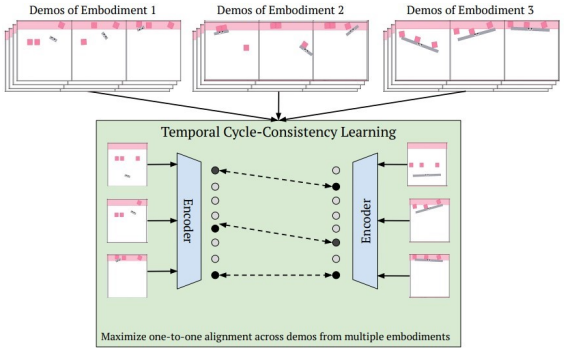

Figure 1.13: Temporal-Cycle Consistency representation, used to learn an embodiment-agnostic encoder in [79]

The correspondence problem between different viewpoints was faced by [30, 72]. In [30] a Convolutional Neural Network was trained by means of a *Triplet-Loss* [83]. The idea was to train a network able to predict an embedding independent from the view-point, but which contains only task relevant features. To reach this objective the network has to produce an embedding, $f(x)$, such that $||f(x_i^a) - f(x_i^p)||_2^2 + \alpha < ||f(x_i^a) - f(x_i^n)||_2^2$ $\forall (f(x_i^a), f(x_i^p), f(x_i^n)) \in \mathcal{T}$, where $\mathcal{T}$ is the set of all possible triplets in the dataset. This means that embedding produced by samples coming from different viewpoints, but that share the same time-step, (x_i^a, x_i^p), should have a similar embedding, while embedding produced by samples coming from the same viewpoint, but in different time-step, (x_i^a, x_i^n), should have a different embedding (Figure 1.14a). In [72], a different approach was used, indeed, a *context translation problem* was solved by means of an Encoder-Decoder architecture (Figure 1.14b). The proposed architecture was trained on pairs of demonstrations, $\mathcal{D}_i = [o_0^i, o_1^i, \dots, o_T^i]$ and $\mathcal{D}_j = [o_0^j, o_1^j, \dots, o_T^j]$ composed of visual observations. Samples in D_i comes from the source context ω_i, while samples in $\mathcal{D}_j$ comes from the target context ω_j. The model must output the observations in D_j conditioned on both $\mathcal{D}_i$ and the first observation o_0^j from the target domain. As it will be explained next, the output of both the Time-Contrastive and the Context-Translation network can be used to obtain an engineered reward function.

Concerning the way how the policy can be obtained, it is necessary to distinguish between Model-Based and Model-Free methods.
Among **Model-Free** methods, a further classification must be made between methods based on *Reward Engineering* and *Adversarial Learning*.
Methods based on Reward Engineering are [72, 30, 77, 79], in which a hand-designed reward function is used to train a RL agent. In particular, the reward functions obtained in the cited works leverage some sort of *Feature Tracking*. In [72] the reward function was $R(o_t^l) = -||Enc_1(o_t^l) - \frac{1}{n}\sum_i^n F(o_t^i, o_0^l)||_2^2 - w_{rec}(||o_t^l - \frac{1}{n}\sum_i^n M(o_t^i, o_0^l)||_2^2)$. The first term is the classic Feature Tracking reward function, where the goal is to minimize the Euclidian Distance between the encoding of the current learner observation o_t^l and the encoding of the demonstration in the learner context, the second term has the aim to penalize the policy for experiencing observations that differ from the translated observation. In [30], the reward function was $R(\mathbf{v}_t, \mathbf{w}_t) = -\alpha|| \mathbf{w}_t - \mathbf{v}_t ||_2^2 - \beta\sqrt{\gamma + || \mathbf{w}_t - \mathbf{v}_t ||_2^2}$, where $\mathbf{v}_t$ is the TCN embedding of the video demonstration at timestep t, while $\mathbf{w}_t$

is the TCN embedding produced by the robot observation (Figure 1.14a). In [77], a keypoint-representation is obtained for both current robot observations z_t, and for each frames of the translated demonstration video $\{z_p^E\}_{p=1}^T$. Then, the reward is computed as $R(z_t, z_{t+1}, z^E) = -\lambda_1 \min_p ||z_t - z_p^E|| - \lambda_2 \min_p ||(z_{t+1} - z_t) - (z_{p+1}^E - z_p^E)||$. In [79], the reward function was defined as $R(s_t) = -\frac{1}{k} ||\phi(s_t) - g||_2^2$, where g is the goal embedding, defined as the mean embedding of the last frame of all the demonstration videos in the dataset, while $\phi(s_t)$ is the embedding of the current observation. Experimental results, on simulation data proved that the proposed method can be used to learn tasks from cross-embodiment demonstrations, outperforming baseline [30] in terms of both sample efficiency and performance.
Regarding the methods based on Adversarial Learning, there are [84, 85]. Obviously, these methods are strictly related to the Generative Adversarial Imitation Learning setting. However, with respect to the methods presented in GAIL paragraph (pag. 18), these methods do not assume access to the demonstrator action. Indeed, the goal of the preliminary work [84] was to prove that the Adversarial Learning Setting can be effectively used even without the action information. To prove this hypothesis, the authors performed a series of experiments in simulation for a walking task, where the same RL policy was trained in two contexts, the first, where the Discriminator had access to the (state, action) pair, the second where the Discriminator had access to state only demonstrations. The results obtained did not show a substantial difference between the two settings, supporting the hypothesis that in task learning the essential information is contained in the state.
The next remarkable work was proposed by the authors of [85], that formalized the *GAIfO* algorithm, (Algorithm 7), that is an extension to state-only demonstration of GAIL [66]. The proposed algorithm was used to train a network to solve tasks in simulation environment [71], with both low-dimensional state representation, and visual-state representation. Results with respect to the number of demonstrated trajectories are reported in Figure 1.15. As it can be noted from the results, GAIfO outperforms previous observation based methods [30, 86], in a setting with a low number of expert trajectories. The main drawback of GAIfO is the high number of environmental interactions needed to learn a policy,

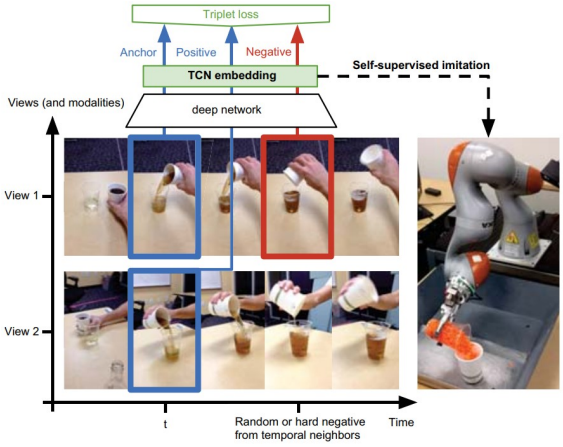

(a) Time-Contrastive network, proposed in [30].

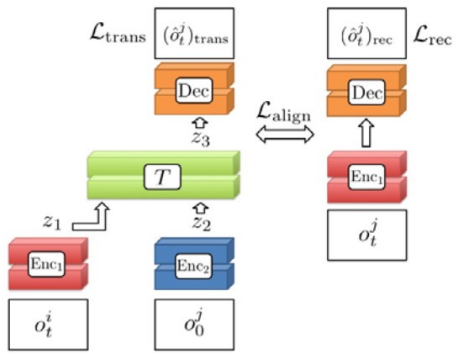

(b) Context-Translation network, proposed in [72]

Figure 1.14: Examples of how the mismatch between demonstrator viewpoint and learner viewpoint can be handled.

since the model-free TRPO [70] algorithm was used to train the policy. This problem was solved by DEALIO [87], which replaced the model-free algorithm with PILQR [88] the model-based RL algorithm reported next.

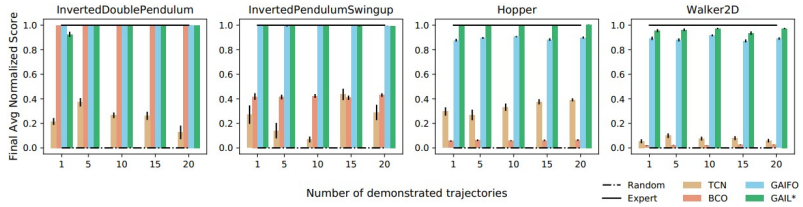

(a) Experimental results in low-dimensional state space

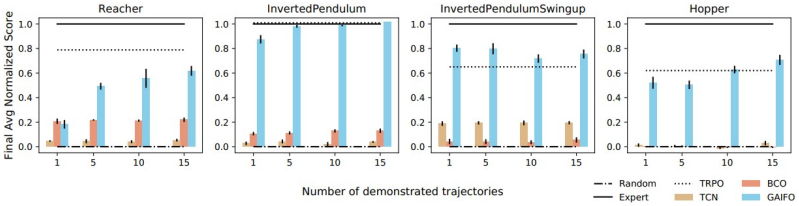

(b) Experimental results in high-dimensional state space

Figure 1.15: Experimental results reported in [85].

Among the **Model-Based** methods a further classification has to be made between methods that obtain the *Inverse Dynamic Model* and methods that obtain the *Forward Dynamic Model*. The former, given in input a transition (s_t, s_{t+1}), obtain a function M, able to map state transition to action i.e., $a_t = M(s_t, s_{t+1})$. While the latter, given in input a state-action pair (s_t, a_t), aim to learn a function F able to generate the next state s_{t+1}, i.e., $s_{t+1} = T(s_t, a_t)$.
Methods that obtain the Inverse Dynamic Model are [89, 86, 90, 91]. In [89] the goal was to obtain a system capable of tying the knot to a rope. To achieve it, a self-supervised learning approach was used to train a Convolutional Neural Network, that, taken in input a pair of images (I_t, I_{t+1}) representing two successive rope states, was able to obtain the action to perform in order to reach the state I_{t+1} from I_t. To train the proposed network, a dataset composed of 30K tuples (I_t, a_t, I_{t+1}) was collected by means of an exploratory policy. Authors in [86] proposed a general approach, depicted in Figure 1.16, and composed by two main parts, the learned Inverse Dynamic Model, M_θ, and the learned policy π_ϕ. In its general form, the learning procedure is an iterative procedure, where the model M_θ^i is updated by maximizing the probability $p_\theta(a_t|s_t, s_{t+1})$, where the tuples (s_t, a_t, s_{t+1}) are collected by running the current policy. Once the dynamic model is updated then it is used to infer the action $\tilde{a}_t$ given the demonstrations. At the end, since the policy has access to

Algorithm 7 GAIfO algorithm [85]

Require: Initial policy π_ϕ^L, Initial Discriminator D_θ
Require: State-only expert demonstration trajectories $\tau^E = \{(s, s')\}$
  while Policy Improves **do**
    Execute π_ϕ^L and collect state transitions $\tau^L = \{(s, s')\}$
    Update D_θ, with $\mathcal{L}_{D_\theta} = -\ (\ \mathbb{E}_{\tau^L}[\log(D_\theta(s, s'))] + \mathbb{E}_{\tau^E}[\log(1 - D_\theta(s, s'))]\ )$
    Update π_ϕ^L, with reward $r_{\pi_\phi^L} = -\ (\ \mathbb{E}_{\tau^L}[\log(D_\theta(s, s'))]\ )$
  end while

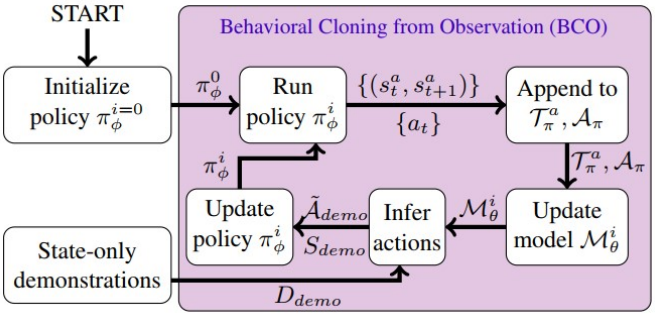

Figure 1.16: Representation of the learning procedure proposed by [86]

both state and action information, classic BC learning can be run, optimizing the policy parameters through maximum-likelihood estimation $\phi^* = \underset{\phi}{argmax} \prod_{i=0}^{N} \pi_\phi^L(\tilde{a}_i|s_i)$. In [90], the same approach as in [86], but the agent's policy was trained according to a linear combination of Behavioral Cloning and Advantage Actor Critic (A2C) objective function [92], i.e., $\mathcal{L}_\theta^{hyb} = \mathbb{E}_{s,a}[A(s)\log(a|s;\theta) + \alpha\ \mathcal{H}(\pi^L(.|s))] + \mathbb{E}_{(\hat{s}_t,\hat{s}_{t+1})\sim D}[\log(\pi^L(M(\hat{s}_t,\hat{s}_{t+1})|\theta)]$. Here, the main problem is the assumption to have access to reward function, which can reduce its applicability in real-robot manipulation tasks. In [91], the work in [93] was extended to state-only demonstration, and the *State-Only Imitation Learning* (SOIL) algorithm was proposed. The context is the one of complex dexterous manipulation, i.e., a simulated humanoid hand must be able to perform tasks such as object reallocation, tool use, in-hand manipulation, and door opening. A neural network was trained to represent the Inverse Dynamic Model, by minimizing the L2-loss, given in input the action performed during the policy rollout. Then, the policy was updated according to *Demo Augmented Policy Gradient* (DAPG) [93], adapted for state-only demonstration, i.e., $g_{SOIL} = g + \lambda_0\ \lambda_1^k\ \sum_{(s_t,\tilde{a}_t\in D')} \nabla_\theta \log \pi_\theta^L(\tilde{a}_t, s_t)$, where g is the Natural Policy Gradient term. The idea is to leverage the demonstrations at the beginning of the training, then exploit the RL algorithm to improve the behavior itself. Indeed, experiments performed in simulation, proved that, with respect to pure RL, the proposed method converges faster, and producing more human-like behaviors.

Methods that obtain the Forward Dynamic Model are [29, 87]. In [29], once the human video demonstration has been translated into the corresponding robot video, the policy was learned according to the model-based RL algorithm SOLARIS [94], which allows to obtain a controller optimized according to Linear-Quadratic Regulator (LQR) procedure. The idea was to optimize the policy in a low-dimensional high-regularized *latent space*, generated according to Variational Inference [95]. Starting from a sequence of observation-action, a Global Dynamic Model over latent trajectory is obtained. Then, given the Latent Dynamic Model, a Linear-Gaussian Controller is obtained through LQR-FLM [64]. Real world robotic experiments, shown that with **2 hours** of robot interaction it was possible to outperform previous works such as [30, 86] and classic BC algorithm, on tasks such as "coffee making" (Figure 1.12) and cup-retrieving (i.e., the robot has to take a cup from a closed drawer). In [87] the sample-inefficiency problem of GAIfO [85] was addressed. The idea was to exploit the adversarial learning setting with state-only demonstration, which has shown promising results (Figure 1.15), and combining it with a more data-efficient RL algorithm, such as PILQR [88]. The core of PILQR is the LQR optimization procedure. Generally speaking, it returns a *linear-gaussian controller* (Formula 1.12), that optimizes

a *quadratic-cost function* (Formula 1.13), under the assumption of *linear-gaussian dynamic* (Formula 1.14).

$$\pi(a_t|s_t) = \mathcal{N}(K_t s_t + k_t, S_t) \tag{1.12}$$

$$c(s_t, a_t) = \begin{bmatrix} s_t \\ a_t \end{bmatrix}^T C_t \begin{bmatrix} s_t \\ a_t \end{bmatrix} + \begin{bmatrix} s_t \\ a_t \end{bmatrix}^T c_t + cc_t \tag{1.13}$$

$$s_{t+1} \sim P(s_{t+1}|s_t, a_t) = \mathcal{N}(F_t \begin{bmatrix} s_t \\ a_t \end{bmatrix} + f_t, \Sigma_t) \tag{1.14}$$

In order to use this framework, the linear-gaussian dynamic model was fitted starting from the current policy rollouts, then, to obtain a quadratic cost function as needed by LQR, the dynamic model was used to express the modified discriminator output (Formula 1.15) as function of the pair (s_t, a_t).

$$D_\theta(s_t, s_{t+1}) = \frac{1}{2} \begin{bmatrix} s_t \\ s_{t+1} \end{bmatrix}^T C^{ss}(s_t, s_{t+1}) \begin{bmatrix} s_t \\ s_{t+1} \end{bmatrix} + \begin{bmatrix} s_t \\ s_{t+1} \end{bmatrix}^T c^{ss}(s_t, s_{t+1}) \tag{1.15}$$

Experiments performed in simulation with low-dimensional state space have shown promising results (Figure 1.17b), in terms of sample-efficiency with respect to the GAIfO baseline. However, improvements would be made in order to: **(1)** reduce the variance, in order to make the learning process more reliable, **(2)** increase the overall performance, **(3)** adapt the algorithm to work with real-world robot manipulation tasks.

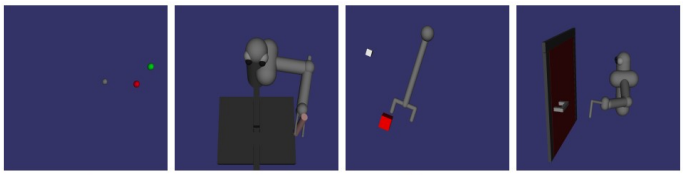

(a) Disc (b) PegInsertion (c) GripperPusher (d) DoorOpening

(a) Control Tasks solved in [87]

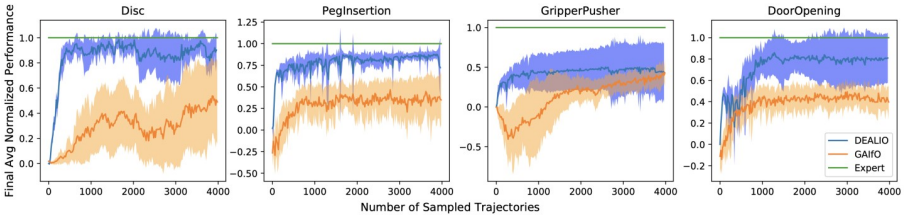

(b) Performance of DEALIO [87] compared against GAIfO [85], with respect to the number of trajectories sampled during the learning process.

Figure 1.17: DEAILO: (1.17a) Control Tasks, (1.17b) Performance Level

Generally, LfO methods have demonstrated interesting features, such as generating a policy from state-based information alone, supporting the hypothesis that the primary source of information for task learning is the sequence of state transitions. Extrapolating the valuable information to perform actions that induce the desired behavior may not be trivial, mainly if the state space is represented by images of a human operator, leading to the design of architectures composed of different stages, which increase not only the complexity of the system itself but also the amount and diversity of data required for their training. In addition, many methods of interest have been tested in simulated or otherwise

relatively simple scenarios, still leaving open the question of whether these methods can be used in real-world complex robotic manipulation tasks.

1.2.4 Summary

This section summarizes all the approaches seen so far, trying to understand their pros and cons. Answering which approaches leads to better performance than the others is not trivial for several reasons ranging from the fact that, as mentioned above, methods are tested in different environments (e.g., some in simulation, others in the real world), on different tasks and using different robotic platforms. It can be said that, by analyzing the state of the art, the most studied approach is Behavioral Cloning. This approach, from a pure implementation point of view, is the simplest, as, in principle, it allows the execution of a purely offline training procedure. Unfortunately, some problems have to be handled, ranging from compounding-error to dataset creation. About the former, some solutions have been proposed, based on interactive learning algorithms, which reduce the covariate-shift phenomena, but introduce the need for active human supervision during the learning. During the past few years, there has been increasing interest in Meta-Learning algorithms, with the ultimate goal of achieving a system that can generalize across different tasks. However, as it turns out, the generalization problem is far from solved. Regarding approaches such as IRL, GAIL, and LfO. Compared to BC, methods such as IRL, GAIL, and LfO are more efficient regarding required demonstrations. However, they introduce RL algorithms into the optimization loop, which requires interaction with the environment, which can be risky and time-consuming. Moreover, despite their promising results, relatively few methods of these three approaches have actually been used in real-world vision-based manipulation tasks, effectively leaving unanswered the question of whether these methods can be used.

Chapter 2

Research Plan

This chapter is dedicated to the presentation of the research project. In Section 2.1, the *Research Topic* will be described. Specifically, starting from the state of the art presented in Section 1.2, which contains a comprehensive overview with respect to the Learning from Demonstration problem, the context of interest will first be identified, going on to describe the application scenario in which the proposed system will be placed. Next, the reference approach currently used to solve the Learning from Demonstration problem given the scenario of interest will be identified. Finally, based on the considerations made earlier, some research gaps will be identified, highlighting how current methods partially solve these gaps and proposing some hints on how advances can be made based on the current state of the literature. In Section 2.2 the *Research Plan* will be described. Specifically, starting from the gaps reported in the previous section, the proposed hints will be formalized, defining hypotheses of methods and procedures that can lead to their implementation, and pointing out why the proposal can improve the current literature. Next, the experimental techniques that will be followed to evaluate and compare the proposed methods will be described.

2.1 Research Topic

In general, this research activity aims to address the problem of Learning from Demonstration, where the goal is to obtain a policy, i.e., a function that maps a sequence of states into the corresponding sequence of actions, from a set of examples. Specifically, with respect to the general problem and the requirements given in Section 1.2, especially the requirement of high-adaptability, the goal is to design a **Vision-based Imitation Learning** system capable of learning the execution of **different tasks**, starting from a set of demonstrations. The resulting policy must be able to infer the current action from a visual observation of the environment from the robot's point of view. Such a system can find applications both in industrial (e.g., ask to a robot to pick a tool and then use it) and social robotic scenarios (e.g., ask to a housecare robot to move an object from one point to another), altough the main focus will be posed on Industrial tasks (e.g., pick-and-place, pushing, peg-insertion). Among the four approaches presented in Section 1.2 the one that is most suitable for the context of interest is *Behavioral Cloning*, in particular those methods that leverage *Meta-Learning* algorithms [47, 49, 48] or in general train a *Multi-Task Imitation Learning* system [5, 4]. From Table 1.2 it can be noted that in terms

of pure success-rate both in the Single-Task and in the Multi-Task Setting the problem is far from being solved, and going from the first setting to the second one is no trivial. Indeed, also in the most "simple" setting, i.e., when instances of the tested task are used during the training, the success rate decreases for almost all the tasks. These results points out the potential of the proposed multi-task imitation learning systems, since, as reported in the works [5, 48], the main reason for the failure of these systems lies in errors in the identification of the critical points of a task and the subsequent execution of the correct action, instead of in the general identification of the intent of the task to be performed, represented for example by the identification of the target object. Starting from this general consideration regarding the state of the art, the current research proposal aims to focus on two closely related aspects, which are described in the paragraph in the following paragraphs.

What is the best representation of the task to facilitate the identification of critical points?

In the works currently proposed in the literature, the dataset is mainly composed of a combination of demonstration videos showing the robot task execution and the action performed by the robot itself, represented by the linear and angular velocity of the end-effector [48] or the desired pose of the end-effector [51, 5]. Regarding the ability to identify critical points within the task, the criticality of the proposed solutions lies in the fact that the visual observations are composed of RGB images and recorded with respect to a third-person viewpoint [48, 5]. With this setting, at least two important critical issues are generated: The first is related to the lack of geometric information, e.g., the relative distance between the gripper and the object being approached. The second is related to the fact that the observations represent a different point of view from that of the robot, which can lead to the creation of occlusions generated by the movement of the arm itself, further complicating the detection of critical points such as the fact that the object is close and therefore the gripper can be closed. With respect to these problems, a possible solution could be to augment the observations by also adding a fourth component represented by the depth image, and also recording the movements from a robot's point of view, for example, by mounting a camera attached the gripper, as is usually done in Vision-Based grasping systems [96].

Moreover, another important aspect related to the task representation is the lack of semantic information that can lead to a correct and meaningful task segmentation. It would be fascinating to obtain a system capable of automatically extracting subtasks from a set of demonstrations of different tasks composed of the same primitives, e.g., approach and push. Current methods [5, 4] have demonstrated a limitation in solving this problem, evidenced especially by the performance decay in the multi-task setting compared to the single-task setting [4, 20], highlighting how training a monolithic architecture that does not explicitly consider task segmentation can lead to performance that is too low for real-world application. Work that has attempted to handle automatic task segmentation has been [49, 54]. Specifically, in [49], a task-phase predictor was trained on a set of primitive demonstrations (e.g., pushing, lifting, placing) based on their length to be used later as a sub-task selector. In [54], a goal-conditioned Variational-Autoencoder was trained to identify an efficient representation of the sub-task to be executed, to be used later for training a conditional policy on that representation. With respect to these methods, and taking inspiration from action-recognition-based methods [97], an alternative approach may be based on using sub-task action labels, then training a multi-task architecture capable of

generating in output both the action for task execution and a label related to the running sub-task that the robot is executing.

What is the best architecture for modeling a policy?
A task demonstration extends over two dimensions, the first is the temporal one, and the second is the spatial one. Different types of architectures have been used in the context of Learning from Demonstration, starting from the classic Convolutional Neural Network [20, 48, 49] up to the modern architectures based on Transformers [51, 4]. From different results reported in [4, 16], it was possible to observe how the use of architectures capable of managing time sequences is crucial to obtain a system with a high success rate. In the context of multi-task learning, however, an additional level must be added, linked to the representation of the tasks and their respective sub-tasks. It is reasonable to think that having an architecture capable of obtaining a representation linked to the sub-tasks performed in the different tasks may lead to greater generalization across the tasks. The architecture closest to this modeling is [54], which uses a conditional Variational Autoencoder to learn a representation of the sub-task starting from the current observation and the observation representative of the final state. In this paper, however, the visual appearance of the proposed tasks was the same, an assumption that may be too strong in a more general context, such as that proposed by [4]. A possible improvement concerning this setting can be represented by the use of Contrastive Loss, used in [30, 79], in order to support the generation of a representation as similar as possible for the same sub-tasks but coming from different contexts and as different as possible for different sub-tasks

2.2 Proposed Research Activity

After the presentation of the context of interest and the aspects to be treated in the current research proposal, this section will formalize the improvement hypotheses reported in Section 2.1, identifying the main methods of interest from which will start the application of the proposed changes, and the procedures that will be used to validate and compare the proposed approach against the state-of-the-art methods.
As discussed in Section 2.1, it was seen that current methods start from a representation of the environment that lacks geometric information and that is obtained from the point of view different from that of the robot, and in particular from that of the end-effector. Concerning this point, starting from the state-of-the-art architecture [4] based on Transformer, the goal will be to extend it in such a way that it will be able to handle time sequences characterized by RGB-D observations, and taken from a camera mounted on the end-effector. Several approaches can be used to achieve this. In fact, in the Computer Vision community, RGB-D images can be handled in different ways. For example, one can apply convolutional layers separately on the RGB and depth images, as in [20], and subsequently perform a fusion between the extracted features based, for example, on their concatenation. Another approach may be using a 3D Point-Cloud Neural Network, such as [98] used in [96]. To answer the question which of the two approaches to prefer, given that the reference method [4] has a transformer-based architecture, a first step may be to apply convolutional filters separately on the RGB and D images and then combine them appropriately, going on to evaluate different fusion techniques, starting from simple concatenation to the use of a weighted sum, with the ultimate goal of generating the embedding as input to the transformer.
This setting will allow evaluating the hypothesis that adding geometric information can

reduce failures caused by collisions with objects of interest or by the inability to determine when to close or open the gripper. The resulting method will then be tested and compared first in simulation, taking advantage of the open-source simulation environments [71, 99]. Then, based on the obtained results, the proposed architecture will be tested and evaluated on a real robot platform, adding an additional experimental contribution that current methods such as [51, 4] lack.
As for the tasks of interest, the main focus will be devoted to industrial tasks (e.g., pick-and-place, push, peg-insertion), introducing an additional constraint with respect to [4], since the system will have to be able to perform real-time inference on low-cost embedded platforms, in order to control a real-world robot platform.
An incremental approach will be used for the design and development of the proposed system. Thus, a single-task setting will first be evaluated, but, with respect to [4], it will be characterized by a high degree of variability based on different initial conditions and different objects to be manipulated so as to evaluate the ability to generalize across a single task, a setting in which meta-learning-based procedures have proven successful [47, 48]. Next, the system will be extended into a multi-task context, where the hypotheses made earlier about using Variational-Autoencoder for learning a representation related to the demonstrated sub-tasks can be evaluated and validated in combinations with the use of Contrastive Loss, which have been shown to be valid in methods such as [30, 79] where the goal has been to learn a task representation from different embodiments [79] and different viewpoints [30]. Here, with respect to [54], the Variational Autoencoder will be combined with Contrastive Loss, to learn a sub-task related representation starting from demonstrations composed of different visual appearance. While, with respect to [4], the proposed combination aims to model explicitly the concept of sub-tasks, which may help the generalization in a multi-task settings by leveraging the task hierarchical structure.

Chapter 3

Other Activities

3.1 Attended Courses

3.1.1 Compulsary Courses

The mandatory courses supported were:

- Scientific Writing and Publishing. The course is focused on presenting the metrics used to assess the goodness of author, paper, and scientific journal. The course ended with the review and comparison of two scientific articles, brought as examples of a well-written and a poorly written article, according to the guidelines presented during the course.
- Advanced Machine Learning. The course aims to present advanced aspects, both theoretical and practical, related to modern Machine Learning techniques. It ended with a project in which a Deep Network was designed, trained and validated to solve the facial attribute multi-class classification problem.
- Optimization Techniques for Engineers. The course aims to present the theoretical aspects needed to model, solve, and evaluate real world problems by leveraging optimization techniques. It ended with a project in which the presented optimization techniques have been used to formulate and solve a trajectory planning problem.
- Computational Paradigms for problem solving. The course presents the Logic Programming paradigm and the Functional Programming paradigm, related to the more general declarative paradigm. During the course, exercises were conducted through which it was possible to analyze and solve problems using the paradigms presented, thus understanding their importance and the main differences from the more well-known Imperative Paradigm.
- English Language C1.

3.1.2 Additional Courses

I decided to add the following two exams to my path:

- Mobile Robots for Critical Mission. The course, related to the Master Degree in Computer Engineering, aims to provide the architectural, methodological, and design elements for the realization of intelligent robots capable of moving autonomously in indoor environment. The course ended with the design, implementation, and validation of a software that allows a mobile robot platform to move autonomously, given the desired start and end points.
- Ottimizzazione. The course aims to present the theoretical aspects related to both continuous and integer linear programming problems, combined with the respective solving algorithms.

Bibliography

[1] Softbank Robotics, "Pepper robot."

[2] Franka Emika, "Franka emika panda robot."

[3] T. Anne, J. Wilkinson, and Z. Li, "Meta-learning for fast adaptive locomotion with uncertainties in environments and robot dynamics," in *2021 IEEE/RSJ International Conference on Intelligent Robots and Systems (IROS)*, pp. 4568–4575, IEEE, 2021.

[4] Z. Mandi, F. Liu, K. Lee, and P. Abbeel, "Towards more generalizable one-shot visual imitation learning," in *2022 International Conference on Robotics and Automation (ICRA)*, pp. 2434–2444, IEEE, 2022.

[5] E. Jang, A. Irpan, M. Khansari, D. Kappler, F. Ebert, C. Lynch, S. Levine, and C. Finn, "Bc-z: Zero-shot task generalization with robotic imitation learning," in *Conference on Robot Learning*, pp. 991–1002, PMLR, 2022.

[6] R. Hafner and M. Riedmiller, "Reinforcement learning in feedback control," *Machine learning*, vol. 84, no. 1, pp. 137–169, 2011.

[7] R. S. Sutton and A. G. Barto, *Reinforcement learning: An introduction*. MIT press, 2018.

[8] B. D. Argall, S. Chernova, M. Veloso, and B. Browning, "A survey of robot learning from demonstration," *Robotics and autonomous systems*, vol. 57, no. 5, pp. 469–483, 2009.

[9] L. P. Kaelbling, M. L. Littman, and A. W. Moore, "Reinforcement learning: A survey," *Journal of artificial intelligence research*, vol. 4, pp. 237–285, 1996.

[10] T. Osa, J. Pajarinen, G. Neumann, J. A. Bagnell, P. Abbeel, J. Peters, *et al.*, "An algorithmic perspective on imitation learning," *Foundations and Trends® in Robotics*, vol. 7, no. 1-2, pp. 1–179, 2018.

[11] G. James, D. Witten, T. Hastie, and R. Tibshirani, *An introduction to statistical learning*, vol. 112. Springer, 2013.

[12] C. Cortes and V. Vapnik, "Support-vector networks," *Machine learning*, vol. 20, no. 3, pp. 273–297, 1995.

[13] S. Kullback and R. A. Leibler, "On information and sufficiency," *The annals of mathematical statistics*, vol. 22, no. 1, pp. 79–86, 1951.

[14] S. Levine, A. Kumar, G. Tucker, and J. Fu, "Offline reinforcement learning: Tutorial, review, and perspectives on open problems," *arXiv preprint arXiv:2005.01643*, 2020.

[15] A. Kumar, J. Hong, A. Singh, and S. Levine, "Should i run offline reinforcement learning or behavioral cloning?," in *International Conference on Learning Representations*, 2021.

[16] A. Mandlekar, D. Xu, J. Wong, S. Nasiriany, C. Wang, R. Kulkarni, L. Fei-Fei, S. Savarese, Y. Zhu, and R. Martín-Martín, "What matters in learning from offline human demonstrations for robot manipulation," in *Conference on Robot Learning*, pp. 1678–1690, PMLR, 2022.

[17] A. Hussein, M. M. Gaber, E. Elyan, and C. Jayne, "Imitation learning: A survey of learning methods," *ACM Computing Surveys (CSUR)*, vol. 50, no. 2, pp. 1–35, 2017.

[18] F. Torabi, G. Warnell, and P. Stone, "Recent advances in imitation learning from observation," in *Proceedings of the Twenty-Eighth International Joint Conference on Artificial Intelligence, IJCAI-19*, pp. 6325–6331, International Joint Conferences on Artificial Intelligence Organization, 7 2019.

[19] F. Codevilla, M. Müller, A. López, V. Koltun, and A. Dosovitskiy, "End-to-end driving via conditional imitation learning," in *2018 IEEE international conference on robotics and automation (ICRA)*, pp. 4693–4700, IEEE, 2018.

[20] T. Zhang, Z. McCarthy, O. Jow, D. Lee, X. Chen, K. Goldberg, and P. Abbeel, "Deep imitation learning for complex manipulation tasks from virtual reality teleoperation," in *2018 IEEE International Conference on Robotics and Automation (ICRA)*, pp. 5628–5635, IEEE, 2018.

[21] G. J. Maeda, G. Neumann, M. Ewerton, R. Lioutikov, O. Kroemer, and J. Peters, "Probabilistic movement primitives for coordination of multiple human–robot collaborative tasks," *Autonomous Robots*, vol. 41, no. 3, pp. 593–612, 2017.

[22] B. Fang, S. Jia, D. Guo, M. Xu, S. Wen, and F. Sun, "Survey of imitation learning for robotic manipulation," *International Journal of Intelligent Robotics and Applications*, vol. 3, no. 4, pp. 362–369, 2019.

[23] O. Kroemer, S. Niekum, and G. Konidaris, "A review of robot learning for manipulation: Challenges, representations, and algorithms," *The Journal of Machine Learning Research*, vol. 22, no. 1, pp. 1395–1476, 2021.

[24] E. Johns, "Coarse-to-fine imitation learning: Robot manipulation from a single demonstration," in *2021 IEEE International Conference on Robotics and Automation (ICRA)*, pp. 4613–4619, IEEE, 2021.

[25] A. Mandlekar, Y. Zhu, A. Garg, J. Booher, M. Spero, A. Tung, J. Gao, J. Emmons, A. Gupta, E. Orbay, *et al.*, "Roboturk: A crowdsourcing platform for robotic skill learning through imitation," in *Conference on Robot Learning*, pp. 879–893, PMLR, 2018.

[26] A. Mandlekar, J. Booher, M. Spero, A. Tung, A. Gupta, Y. Zhu, A. Garg, S. Savarese, and L. Fei-Fei, "Scaling robot supervision to hundreds of hours with roboturk: Robotic manipulation dataset through human reasoning and dexterity," in *2019 IEEE/RSJ International Conference on Intelligent Robots and Systems (IROS)*, pp. 1048–1055, IEEE, 2019.

[27] C. Systems, "Cyberforce."

[28] D. Systems, "Touch," Jun 2020.

[29] L. Smith, N. Dhawan, M. Zhang, P. Abbeel, and S. Levine, "Avid: Learning multi-stage tasks via pixel-level translation of human videos," *arXiv preprint arXiv:1912.04443*, 2019.

[30] P. Sermanet, C. Lynch, Y. Chebotar, J. Hsu, E. Jang, S. Schaal, S. Levine, and G. Brain, "Time-contrastive networks: Self-supervised learning from video," in *2018 IEEE international conference on robotics and automation (ICRA)*, pp. 1134–1141, IEEE, 2018.

[31] H. Liu, C. Zhang, Y. Zhu, C. Jiang, and S.-C. Zhu, "Mirroring without overimitation: Learning functionally equivalent manipulation actions," *Proceedings of the AAAI Conference on Artificial Intelligence*, vol. 33, pp. 8025–8033, Jul. 2019.

[32] H. Liu, X. Xie, M. Millar, M. Edmonds, F. Gao, Y. Zhu, V. J. Santos, B. Rothrock, and S.-C. Zhu, "A glove-based system for studying hand-object manipulation via joint pose and force sensing," in *2017 IEEE/RSJ International Conference on Intelligent Robots and Systems (IROS)*, pp. 6617–6624, IEEE, 2017.

[33] A. Ijspeert, J. Nakanishi, and S. Schaal, "Learning attractor landscapes for learning motor primitives," *Advances in neural information processing systems*, vol. 15, 2002.

[34] A. J. Ijspeert, J. Nakanishi, H. Hoffmann, P. Pastor, and S. Schaal, "Dynamical movement primitives: learning attractor models for motor behaviors," *Neural computation*, vol. 25, no. 2, pp. 328–373, 2013.

[35] F. Meier, E. Theodorou, F. Stulp, and S. Schaal, "Movement segmentation using a primitive library," in *2011 IEEE/RSJ International Conference on Intelligent Robots and Systems*, pp. 3407–3412, IEEE, 2011.

[36] R. Caccavale, M. Saveriano, A. Finzi, and D. Lee, "Kinesthetic teaching and attentional supervision of structured tasks in human–robot interaction," *Autonomous Robots*, vol. 43, no. 6, pp. 1291–1307, 2019.

[37] A. Agostini, M. Saveriano, D. Lee, and J. Piater, "Manipulation planning using object-centered predicates and hierarchical decomposition of contextual actions," *IEEE Robotics and Automation Letters*, vol. 5, no. 4, pp. 5629–5636, 2020.

[38] A. Paraschos, C. Daniel, J. R. Peters, and G. Neumann, "Probabilistic movement primitives," *Advances in neural information processing systems*, vol. 26, 2013.

[39] D. A. Pomerleau, "Alvinn: An autonomous land vehicle in a neural network," *Advances in neural information processing systems*, vol. 1, 1988.

[40] S. Ross and D. Bagnell, "Efficient reductions for imitation learning," in *Proceedings of the thirteenth international conference on artificial intelligence and statistics*, pp. 661–668, JMLR Workshop and Conference Proceedings, 2010.

[41] S. Ross, G. Gordon, and D. Bagnell, "A reduction of imitation learning and structured prediction to no-regret online learning," in *Proceedings of the fourteenth international conference on artificial intelligence and statistics*, pp. 627–635, JMLR Workshop and Conference Proceedings, 2011.

[42] M. Laskey, C. Chuck, J. Lee, J. Mahler, S. Krishnan, K. Jamieson, A. Dragan, and K. Goldberg, "Comparing human-centric and robot-centric sampling for robot deep learning from demonstrations," in *2017 IEEE International Conference on Robotics and Automation (ICRA)*, pp. 358–365, IEEE, 2017.

[43] M. Kelly, C. Sidrane, K. Driggs-Campbell, and M. J. Kochenderfer, "Hg-dagger: Interactive imitation learning with human experts," in *2019 International Conference on Robotics and Automation (ICRA)*, pp. 8077–8083, IEEE, 2019.

[44] A. Mandlekar, D. Xu, R. Martín-Martín, Y. Zhu, L. Fei-Fei, and S. Savarese, "Human-in-the-loop imitation learning using remote teleoperation," *arXiv preprint arXiv:2012.06733*, 2020.

[45] E. Chisari, T. Welschehold, J. Boedecker, W. Burgard, and A. Valada, "Correct me if i am wrong: Interactive learning for robotic manipulation," *IEEE Robotics and Automation Letters*, vol. 7, no. 2, pp. 3695–3702, 2022.

[46] C. Finn, P. Abbeel, and S. Levine, "Model-agnostic meta-learning for fast adaptation of deep networks," in *International conference on machine learning*, pp. 1126–1135, PMLR, 2017.

[47] C. Finn, T. Yu, T. Zhang, P. Abbeel, and S. Levine, "One-shot visual imitation learning via meta-learning," in *Conference on robot learning*, pp. 357–368, PMLR, 2017.

[48] T. Yu, C. Finn, S. Dasari, A. Xie, T. Zhang, P. Abbeel, and S. Levine, "One-shot imitation from observing humans via domain-adaptive meta-learning," in *Proceedings of Robotics: Science and Systems*, (Pittsburgh, Pennsylvania), June 2018.

[49] T. Yu, P. Abbeel, S. Levine, and C. Finn, "One-shot hierarchical imitation learning of compound visuomotor tasks," *arXiv preprint arXiv:1810.11043*, 2018.

[50] Y. Duan, M. Andrychowicz, B. Stadie, O. Jonathan Ho, J. Schneider, I. Sutskever, P. Abbeel, and W. Zaremba, "One-shot imitation learning," *Advances in neural information processing systems*, vol. 30, 2017.

[51] S. Dasari and A. Gupta, "Transformers for one-shot visual imitation," in *Conference on Robot Learning*, pp. 2071–2084, PMLR, 2021.

[52] D. Xu, S. Nair, Y. Zhu, J. Gao, A. Garg, L. Fei-Fei, and S. Savarese, "Neural task programming: Learning to generalize across hierarchical tasks," in *2018 IEEE International Conference on Robotics and Automation (ICRA)*, pp. 3795–3802, IEEE, 2018.

[53] Y. Yang, Y. Li, C. Fermuller, and Y. Aloimonos, "Robot learning manipulation action plans by" watching" unconstrained videos from the world wide web," in *Proceedings of the AAAI Conference on Artificial Intelligence*, vol. 29, 2015.

[54] A. Mandlekar, D. Xu, R. Martín-Martín, S. Savarese, and L. Fei-Fei, "Gti: Learning to generalize across long-horizon tasks from human demonstrations," in *Proceedings of Robotics: Science and Systems*, (Corvalis, Oregon, USA), July 2020.

[55] D. B. Grimes and R. P. Rao, "Learning actions through imitation and exploration: Towards humanoid robots that learn from humans," in *Creating Brain-Like Intelligence*, pp. 103–138, Springer, 2009.

[56] P. Englert, A. Paraschos, M. P. Deisenroth, and J. Peters, "Probabilistic model-based imitation learning," *Adaptive Behavior*, vol. 21, no. 5, pp. 388–403, 2013.

[57] M. P. Deisenroth, P. Englert, J. Peters, and D. Fox, "Multi-task policy search for robotics," in *2014 IEEE international conference on robotics and automation (ICRA)*, pp. 3876–3881, IEEE, 2014.

[58] P. Abbeel and A. Y. Ng, "Apprenticeship learning via inverse reinforcement learning," in *Proceedings of the twenty-first international conference on Machine learning*, p. 1, 2004.

[59] N. D. Ratliff, J. A. Bagnell, and M. A. Zinkevich, "Maximum margin planning," in *Proceedings of the 23rd international conference on Machine learning*, pp. 729–736, 2006.

[60] B. D. Ziebart, A. L. Maas, J. A. Bagnell, A. K. Dey, *et al.*, "Maximum entropy inverse reinforcement learning.," in *Aaai*, vol. 8, pp. 1433–1438, Chicago, IL, USA, 2008.

[61] N. D. Ratliff, D. Silver, and J. A. Bagnell, "Learning to search: Functional gradient techniques for imitation learning," *Autonomous Robots*, vol. 27, no. 1, pp. 25–53, 2009.

[62] M. Wulfmeier, P. Ondruska, and I. Posner, "Maximum entropy deep inverse reinforcement learning," *arXiv preprint arXiv:1507.04888*, 2015.

[63] C. Finn, S. Levine, and P. Abbeel, "Guided cost learning: Deep inverse optimal control via policy optimization," in *International conference on machine learning*, pp. 49–58, PMLR, 2016.

[64] S. Levine and P. Abbeel, "Learning neural network policies with guided policy search under unknown dynamics," *Advances in neural information processing systems*, vol. 27, 2014.

[65] N. Das, S. Bechtle, T. Davchev, D. Jayaraman, A. Rai, and F. Meier, "Model-based inverse reinforcement learning from visual demonstrations," in *Conference on Robot Learning*, pp. 1930–1942, PMLR, 2021.

[66] J. Ho and S. Ermon, "Generative adversarial imitation learning," *Advances in neural information processing systems*, vol. 29, 2016.

[67] I. Kostrikov, K. K. Agrawal, D. Dwibedi, S. Levine, and J. Tompson, "Discriminator-actor-critic: Addressing sample inefficiency and reward bias in adversarial imitation learning," in *International Conference on Learning Representations*, 2018.

[68] J. Fu, K. Luo, and S. Levine, "Learning robust rewards with adverserial inverse reinforcement learning," in *International Conference on Learning Representations*, 2018.

[69] S. K. S. Ghasemipour, R. Zemel, and S. Gu, "A divergence minimization perspective on imitation learning methods," in *Conference on Robot Learning*, pp. 1259–1277, PMLR, 2020.

[70] J. Schulman, S. Levine, P. Abbeel, M. Jordan, and P. Moritz, "Trust region policy optimization," in *International conference on machine learning*, pp. 1889–1897, PMLR, 2015.

[71] G. Brockman, V. Cheung, L. Pettersson, J. Schneider, J. Schulman, J. Tang, and W. Zaremba, "Openai gym," *arXiv preprint arXiv:1606.01540*, 2016.

[72] Y. Liu, A. Gupta, P. Abbeel, and S. Levine, "Imitation from observation: Learning to imitate behaviors from raw video via context translation," in *2018 IEEE International Conference on Robotics and Automation (ICRA)*, pp. 1118–1125, IEEE, 2018.

[73] S. Reddy, A. D. Dragan, and S. Levine, "Sqil: Imitation learning via reinforcement learning with sparse rewards," in *International Conference on Learning Representations*, 2019.

[74] K. Zolna, S. Reed, A. Novikov, S. G. Colmenarejo, D. Budden, S. Cabi, M. Denil, N. de Freitas, and Z. Wang, "Task-relevant adversarial imitation learning," in *Conference on Robot Learning*, pp. 247–263, PMLR, 2021.

[75] R. Rafailov, T. Yu, A. Rajeswaran, and C. Finn, "Visual adversarial imitation learning using variational models," *Advances in Neural Information Processing Systems*, vol. 34, pp. 3016–3028, 2021.

[76] G. Barth-Maron, M. W. Hoffman, D. Budden, W. Dabney, D. Horgan, D. Tb, A. Muldal, N. Heess, and T. Lillicrap, "Distributed distributional deterministic policy gradients," *arXiv preprint arXiv:1804.08617*, 2018.

[77] H. Xiong, Q. Li, Y.-C. Chen, H. Bharadhwaj, S. Sinha, and A. Garg, "Learning by watching: Physical imitation of manipulation skills from human videos," in *2021 IEEE/RSJ International Conference on Intelligent Robots and Systems (IROS)*, pp. 7827–7834, IEEE, 2021.

[78] J. Li, T. Lu, X. Cao, Y. Cai, and S. Wang, "Meta-imitation learning by watching video demonstrations," in *International Conference on Learning Representations*, 2021.

[79] K. Zakka, A. Zeng, P. Florence, J. Tompson, J. Bohg, and D. Dwibedi, "Xirl: Cross-embodiment inverse reinforcement learning," in *Conference on Robot Learning*, pp. 537–546, PMLR, 2022.

[80] D. Dwibedi, Y. Aytar, J. Tompson, P. Sermanet, and A. Zisserman, "Temporal cycle-consistency learning," in *Proceedings of the IEEE/CVF conference on computer vision and pattern recognition*, pp. 1801–1810, 2019.

[81] J.-Y. Zhu, T. Park, P. Isola, and A. A. Efros, "Unpaired image-to-image translation using cycle-consistent adversarial networks," in *Proceedings of the IEEE international conference on computer vision*, pp. 2223–2232, 2017.

[82] X. Huang, M.-Y. Liu, S. Belongie, and J. Kautz, "Multimodal unsupervised image-to-image translation," in *Proceedings of the European conference on computer vision (ECCV)*, pp. 172–189, 2018.

[83] F. Schroff, D. Kalenichenko, and J. Philbin, "Facenet: A unified embedding for face recognition and clustering," in *Proceedings of the IEEE conference on computer vision and pattern recognition*, pp. 815–823, 2015.

[84] J. Merel, Y. Tassa, D. TB, S. Srinivasan, J. Lemmon, Z. Wang, G. Wayne, and N. Heess, "Learning human behaviors from motion capture by adversarial imitation," *arXiv preprint arXiv:1707.02201*, 2017.

[85] F. Torabi, G. Warnell, and P. Stone, "Generative adversarial imitation from observation," *arXiv preprint arXiv:1807.06158*, 2018.

[86] F. Torabi, G. Warnell, and P. Stone, "Behavioral cloning from observation," in *Proceedings of the 27th International Joint Conference on Artificial Intelligence*, pp. 4950–4957, 2018.

[87] F. Torabi, G. Warnell, and P. Stone, "Dealio: Data-efficient adversarial learning for imitation from observation," in *2021 IEEE/RSJ International Conference on Intelligent Robots and Systems (IROS)*, pp. 2391–2397, IEEE, 2021.

[88] Y. Chebotar, K. Hausman, M. Zhang, G. Sukhatme, S. Schaal, and S. Levine, "Combining model-based and model-free updates for trajectory-centric reinforcement learning," in *International conference on machine learning*, pp. 703–711, PMLR, 2017.

[89] A. Nair, D. Chen, P. Agrawal, P. Isola, P. Abbeel, J. Malik, and S. Levine, "Combining self-supervised learning and imitation for vision-based rope manipulation," in *2017 IEEE international conference on robotics and automation (ICRA)*, pp. 2146–2153, IEEE, 2017.

[90] X. Guo, S. Chang, M. Yu, G. Tesauro, and M. Campbell, "Hybrid reinforcement learning with expert state sequences," in *Proceedings of the AAAI Conference on Artificial Intelligence*, vol. 33, pp. 3739–3746, 2019.

[91] I. Radosavovic, X. Wang, L. Pinto, and J. Malik, "State-only imitation learning for dexterous manipulation," in *2021 IEEE/RSJ International Conference on Intelligent Robots and Systems (IROS)*, pp. 7865–7871, IEEE, 2021.

[92] V. Mnih, A. P. Badia, M. Mirza, A. Graves, T. Lillicrap, T. Harley, D. Silver, and K. Kavukcuoglu, "Asynchronous methods for deep reinforcement learning," in *International conference on machine learning*, pp. 1928–1937, PMLR, 2016.

[93] A. Rajeswaran, V. Kumar, A. Gupta, G. Vezzani, J. Schulman, E. Todorov, and S. Levine, "Learning complex dexterous manipulation with deep reinforcement learning and demonstrations," in *Proceedings of Robotics: Science and Systems*, (Pittsburgh, Pennsylvania), June 2018.

[94] M. Zhang, S. Vikram, L. Smith, P. Abbeel, M. Johnson, and S. Levine, "Solar: Deep structured representations for model-based reinforcement learning," in *International Conference on Machine Learning*, pp. 7444–7453, PMLR, 2019.

[95] D. P. Kingma and M. Welling, "Auto-Encoding Variational Bayes," in *2nd International Conference on Learning Representations, ICLR 2014, Banff, AB, Canada, April 14-16, 2014, Conference Track Proceedings*, 2014.

[96] H.-S. Fang, C. Wang, M. Gou, and C. Lu, "Graspnet-1billion: A large-scale benchmark for general object grasping," in *Proceedings of the IEEE/CVF Conference on Computer Vision and Pattern Recognition*, pp. 11444–11453, 2020.

[97] R. Goyal, S. Ebrahimi Kahou, V. Michalski, J. Materzynska, S. Westphal, H. Kim, V. Haenel, I. Fruend, P. Yianilos, M. Mueller-Freitag, *et al.*, "The" something something" video database for learning and evaluating visual common sense," in *Proceedings of the IEEE international conference on computer vision*, pp. 5842–5850, 2017.

[98] C. R. Qi, L. Yi, H. Su, and L. J. Guibas, "Pointnet++: Deep hierarchical feature learning on point sets in a metric space," *Advances in neural information processing systems*, vol. 30, 2017.

[99] Y. Zhu, J. Wong, A. Mandlekar, and R. Martín-Martín, "robosuite: A modular simulation framework and benchmark for robot learning," *arXiv preprint arXiv:2009.12293*, 2020.